Attachment 18

LR-N06-0286
LCR H05-01, Rev. 1

HOPE CREEK GENERATING STATION
FACILITY OPERATING LICENSE NPF-57
DOCKET NO. 50-354

REQUEST FOR LICENSE AMENDMENT
EXTENDED POWER UPRATE

Hydrodynamic Loads on Hope Creek Unit 1 Steam Dryer to 200 Hz
CDI Report 06-17, Revision 2
September 2006

C.D.I. Report No. 06-17

Hydrodynamic Loads on Hope Creek Unit 1 Steam Dryer to 200 Hz

Revision 2

Prepared by

Continuum Dynamics, Inc.
34 Lexington Avenue
Ewing, NJ 08618

Prepared under Purchase Order No. 4500341046 for

Nuclear Business Unit, PSEG Nuclear LLC
Materials Center, Alloway Creek Neck Road
Hancocks Bridge, NJ 08038

Approved by

Alan Bilanin

Alan J. Bilanin

September 2006

Executive Summary

Measured in-plant pressure time-history data in the four main steam lines of Hope Creek Unit 1 (HC1), at the eight strain gage locations at Current Licensed Thermal Power (CLTP), are processed by a dynamic model of the steam delivery system to predict loads on the steam dryer. These measured data are used with a validated acoustic circuit model to predict the fluctuating pressures anticipated across components of the steam dryer in the reactor vessel. The hydrodynamic load data may then be used by a structural analyst to assess the structural adequacy of the steam dryer in HC1.

Additional measured 1/8th scale pressure time-history data, at CLTP and Extended Power Uprate (EPU), are converted to full-scale pressure time-history data and used to predict hydrodynamic loads on the steam dryer as well.

This effort provides PSEG with a dryer dynamic load definition that comes directly from measured in-plant data and subscale test data, and the application of a validated acoustic circuit model, at power levels where the pressure data were acquired.

Table of Contents

Section		Page
	Executive Summary	i
	Table of Contents	ii
1.	Introduction	1
2.	Modeling Considerations	2
	2.1 Helmholtz Analysis	2
	2.2 Acoustic Circuit Analysis	3
3.	Input Pressure Data	5
	3.1 In-Plant CLTP	5
	3.2 In-Plant Conservatism	9
	3.3 Subscale CLTP and EPU	10
4.	Results	22
	4.1 In-Plant CLTP	22
	4.2 In-Plant Conservatism	22
	4.3 Subscale CLTP and EPU	22
5.	Conclusions	36
6.	References	37

1. Introduction

In Spring 2005 Exelon installed new steam dryers into Quad Cities Unit 2 (QC2) and Quad Cities Unit 1. This replacement design, developed by General Electric, sought to improve dryer performance and overcome structural inadequacies identified on the original dryers, which had been in place for the last 30 years. As a means for confirming the adequacy of the steam dryer, the QC2 dryer was instrumented with pressure sensors at 27 locations. These pressures formed the set of data used to validate the predictions of an acoustic circuit model under development by Continuum Dynamics, Inc. for several years [1]. The results of this benchmark exercise [2] confirmed the predictive ability of the acoustic circuit model for pressure loading across the dryer. This model, validated against the Exelon full scale data, is used in this effort.

This report applies this validated acoustic circuit model to the Hope Creek Unit 1 (HC1) steam dryer and main steam line geometry. Data obtained from the four main steam lines are used to generate predictions of the pressure loading on the HC1 dryer at Current Licensed Thermal Power (CLTP). In addition, data obtained from a 1/8th scale model of the HC1 steam delivery system are used to generate full-scale predictions of the pressure loading on the HC1 dryer at CLTP and at Extended Power Uprate (EPU).

2. Modeling Considerations

The HC1 steam supply system is broken into two distinct analyses: a Helmholtz solution within the steam dome and an acoustic circuit analysis in the main steam lines. This section of the report highlights the two approaches taken here.

2.1 Helmholtz Analysis

A cross-section of the steam dome (and steam dryer) is shown below in Figure 2.1, with HC1 dimensions as shown. The complex three-dimensional geometry is rendered onto a uniformly-spaced rectangular grid (with mesh spacing of approximately 1.5 inches), and a solution is obtained for the Helmholtz equation

$$\frac{\partial^2 P}{\partial x^2}+\frac{\partial^2 P}{\partial y^2}+\frac{\partial^2 P}{\partial z^2}+\frac{\omega^2}{a^2}P=\nabla^2 P+\frac{\omega^2}{a^2}P=0$$

where P is the pressure at a grid point, ω is frequency, and a is acoustic speed in steam.

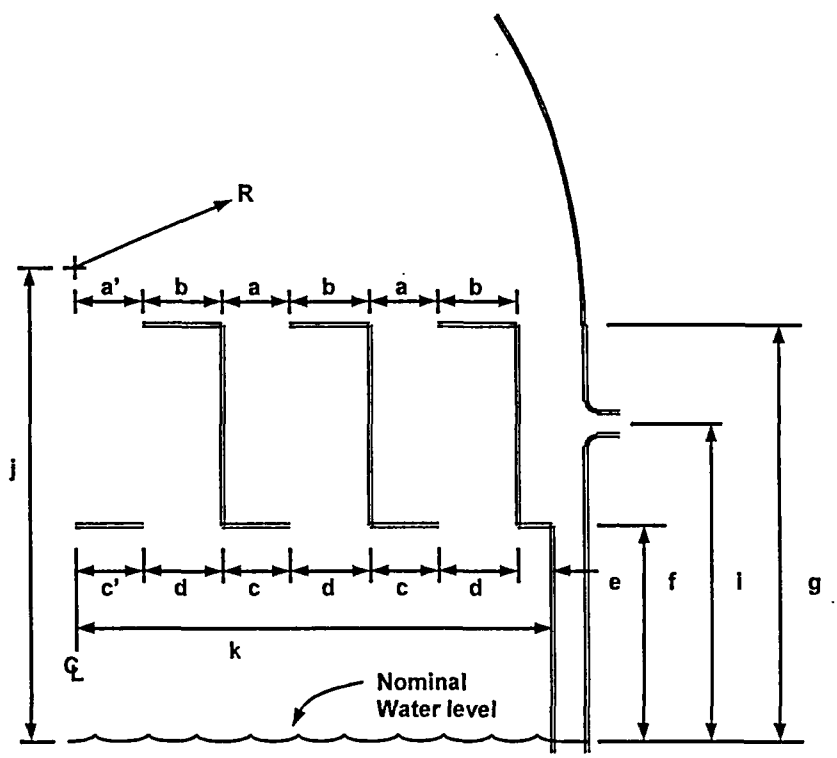

Figure 2.1. Cross-sectional description of the steam dome and dryer, with the verified HC1 dimensions of a' = 15.0, a = 17.5 in, b = 13.5 in, c' = 21.0 in, c = 15.0 in, d = 16.0 in, e = 21.0 in, f = 73.0 in, g = 163.0 in, i = 96.5 in, j = 183.0 in, k = 120.0 in, and R = 125.5 in.

This equation is solved for incremental frequencies from 0 to 200 Hz, subject to the boundary conditions

$$\frac{dP}{dn} = 0$$

normal to all solid surfaces (the steam dome wall and interior and exterior surfaces of the dryer),

$$\frac{dP}{dn} \propto \frac{i\omega}{a} P$$

normal to the nominal water level surface, and unit pressure applied to one inlet to a main steam line and zero applied to the other three.

2.2 Acoustic Circuit Analysis

The Helmholtz solution within the steam dome is coupled to an acoustic circuit solution in the main steam lines. Pulsations in a single-phase compressible medium, where acoustic wavelengths are long compared to component dimensions, and in particular long compared to transverse dimensions (directions perpendicular to the primary flow directions), lend themselves to application of the acoustic circuit methodology. If the analysis is restricted to frequencies below 200 Hz, acoustic wavelengths are approximately 8 feet in length and wavelengths are therefore long compared to most components of interest, such as branch junctions.

Acoustic circuit analysis divides the main steam lines into elements which are each characterized, as sketched in Figure 2.2, by a length L, a cross-sectional area A, a fluid mean density $\bar{\rho}$, a fluid mean flow velocity $\bar{U}$, and a fluid mean acoustic speed $\bar{a}$.

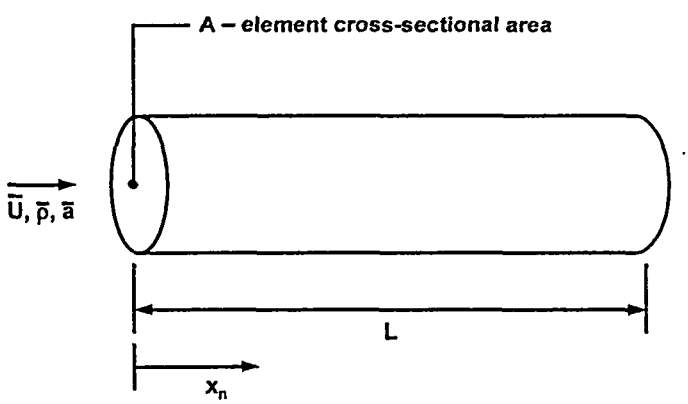

Figure 2.2. Schematic of an element in the acoustic circuit analysis, with length L and cross-sectional area A.

Application of acoustic circuit methodology generates solutions for the fluctuating pressure P_n and velocity u_n in the nth element of the form

$$P_n = \left[A_n e^{ik_{1n}x_n} + B_n e^{ik_{2n}x_n}\right] e^{i\omega t}$$

$$u_n = -\frac{1}{\rho \bar{a}^2}\left[\frac{(\omega + \bar{U}_n k_{1n})}{k_{1n}} A_n e^{ik_{1n}x_n} + \frac{(\omega + \bar{U}_n k_{2n})}{k_{2n}} B_n e^{ik_{2n}x_n}\right] e^{i\omega t}$$

where harmonic time dependence of the form $e^{i\omega t}$ has been assumed. The wave numbers k_{1n} and k_{2n} are the two complex roots of the equation

$$k_n^{\,2} + i\frac{f_n\left|\bar{U}_n\right|}{D_n \bar{a}^2}(\omega + \bar{U}_n k_n) - \frac{1}{\bar{a}^2}(\omega + \bar{U}_n k_n)^2 = 0$$

where f_n is the pipe friction factor for element n, D_n is the hydrodynamic diameter for element n, and $i = \sqrt{-1}$. A_n and B_n are complex constants which are a function of frequency and are determined by satisfying continuity of pressure and mass conservation at element junctions.

The main steam line piping geometry is summarized in Table 2.1.

Table 2.1. Main steam line lengths at HC1. The main steam lines are 26 inch Schedule 80 (ID = 23.647 in) to the strain gages.

Main Steam Line	Distance to First Strain Gage (ft)	Distance to Second Strain Gage (ft)
A	9.71	45.83
B	9.71	45.71
C	9.71	45.71
D	9.71	45.83

3. Input Pressure Data

3.1 In-Plant CLTP

Strain gages were mounted on the four main steam lines. The in-plant data examined here are summarized in Table 3.1, and include eight strain gage measurements. Recorded strain is converted to pressure

$$P = 3.17\ \varepsilon_h$$

where P is the pressure in psid and ε_h is the hoop strain in $\mu\varepsilon$ [3].

Table 3.1. Data set considered for HC1.

Data Set	Feed Flow (10^6 lbs/hr)	Data Rate (samples/sec)	Pertinent Comments
20060511105519	14.40	1024	CLTP

Because of the failure of the lower C and D main steam line strain gages, symmetry of the steam lines were used as a justification to replace these signals with those on main steam lines B and A, respectively. Geometry considerations support this substitution with regard to main steam line length (Table 2.1) and standpipe locations (Table 3.2). However, phasing information is generally lost when main steam line history signals are replaced.

It is therefore important to shift the phase of the time signal on main steam lines C and D to maximize the load on the dryer, resulting in a conservative load prediction. This step was accomplished by shifting the time from main steam line C, then from main steam line D, then back to main steam line C until the maximum load on the dryer was achieved. This maximum low resolution load then established the phase of the signals on the C and D lines to maximize the dryer loading.

Table 3.2. Standpipe location summary at HC1.

Main Steam Line	Distances From Upstream Elbow (ft)
A	5.09, 8.15, 11.21
B	6.95, 10.11, 17.90, 21.06, 24.21
C	6.94, 10.10, 17.72, 22.99
D	5.09, 8.15, 11.21

Figures 3.1 and 3.2 provide the power spectral density (PSD) of the useful strain gages (converted to pressure) on main steam lines A and B, while Table 3.3 summarizes the pressure levels recorded in the main steam lines. Further, it can be shown [2] that these signals can be modified by the coherence of the signals between the upper and lower strain gages on each line. This coherence is shown in Figure 3.3, and applied to the signals shown in Figures 3.1 and 3.2.

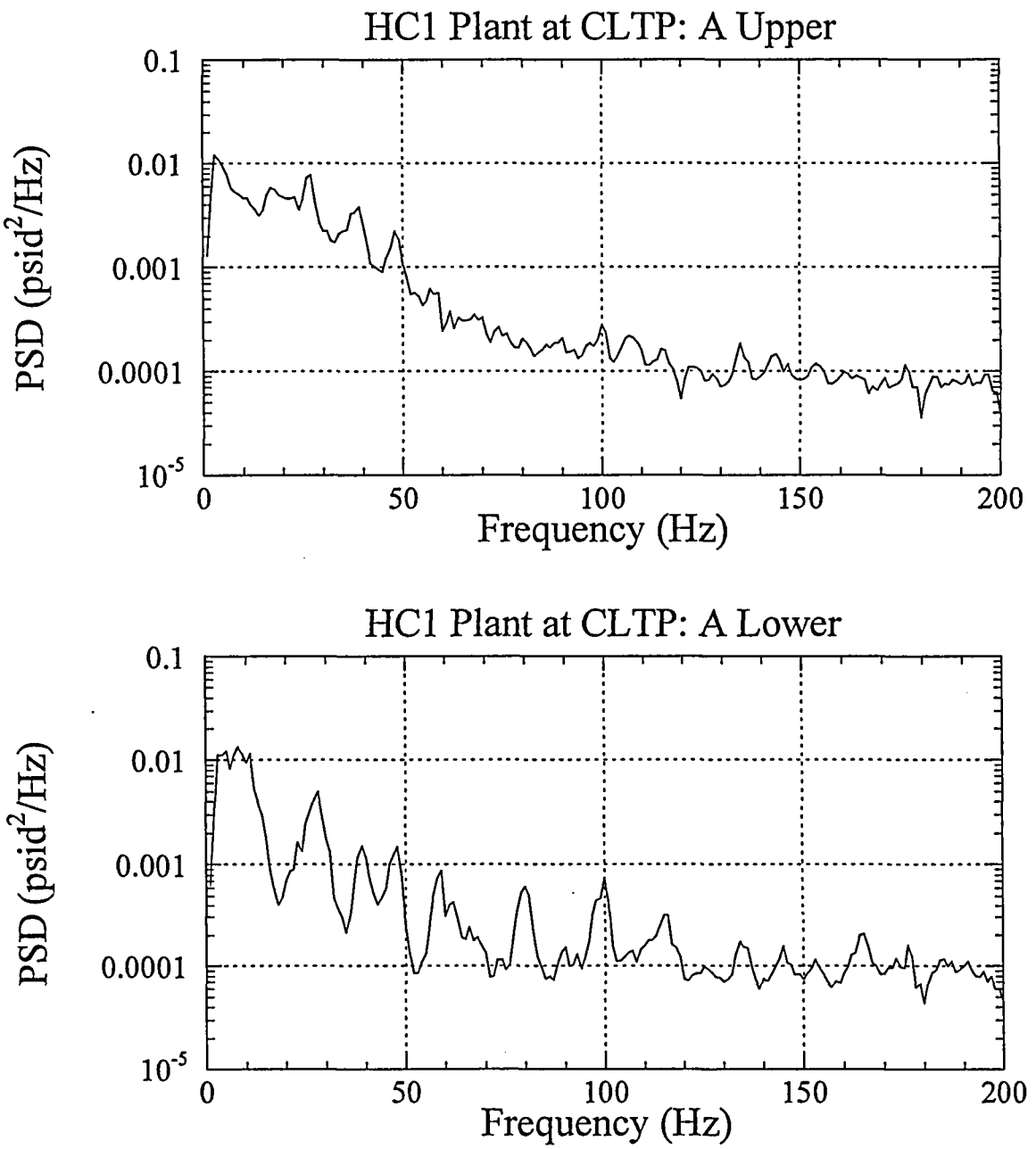

Figure 3.1. PSD comparison of strain gage data at CLTP power, converted to pressure, for main steam line A: upstream strain gage (top) and downstream strain gage (bottom).

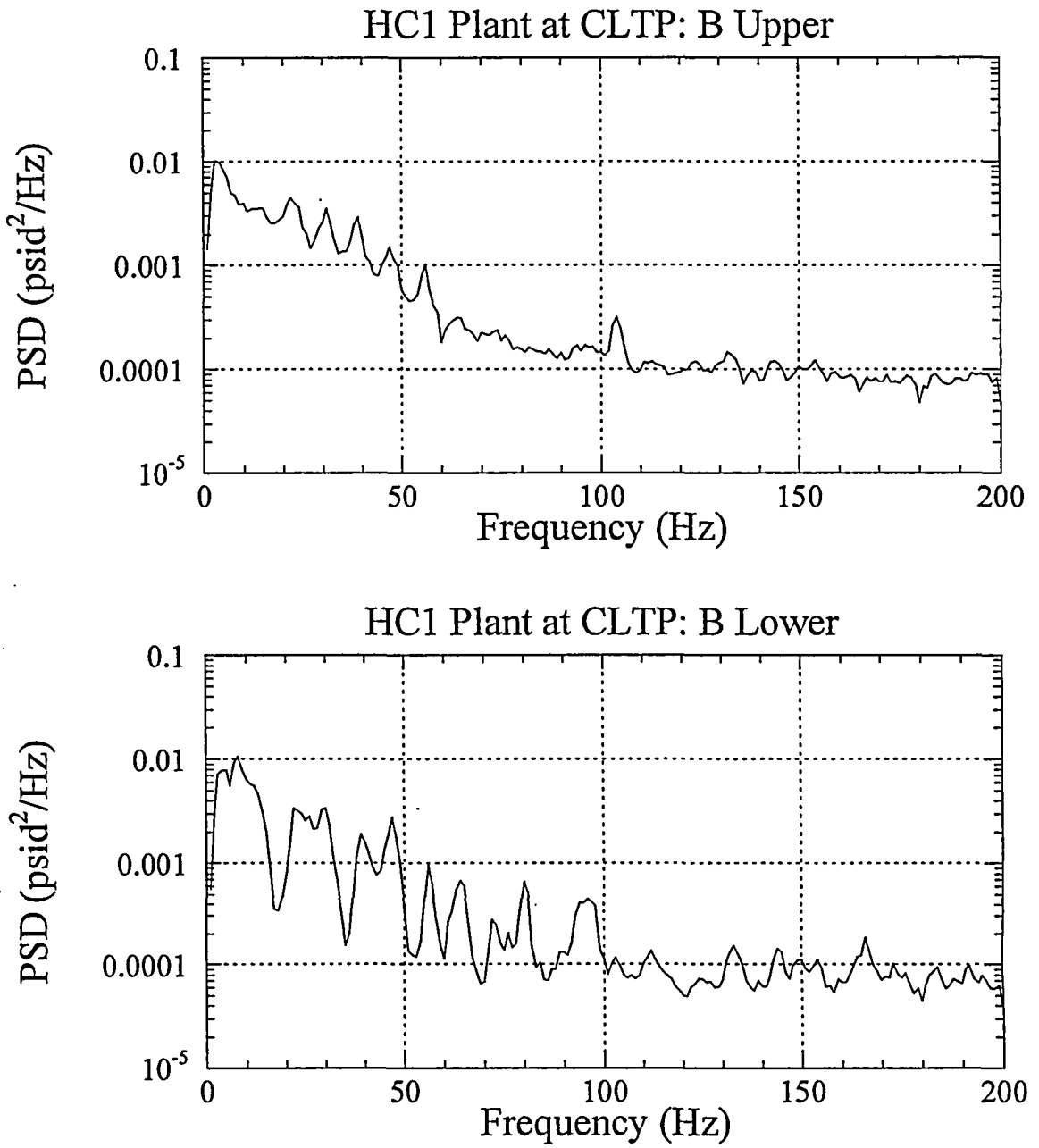

Figure 3.2. PSD comparison of strain gage data at CLTP power, converted to pressure, for main steam line B: upstream strain gage (top) and downstream strain gage (bottom).

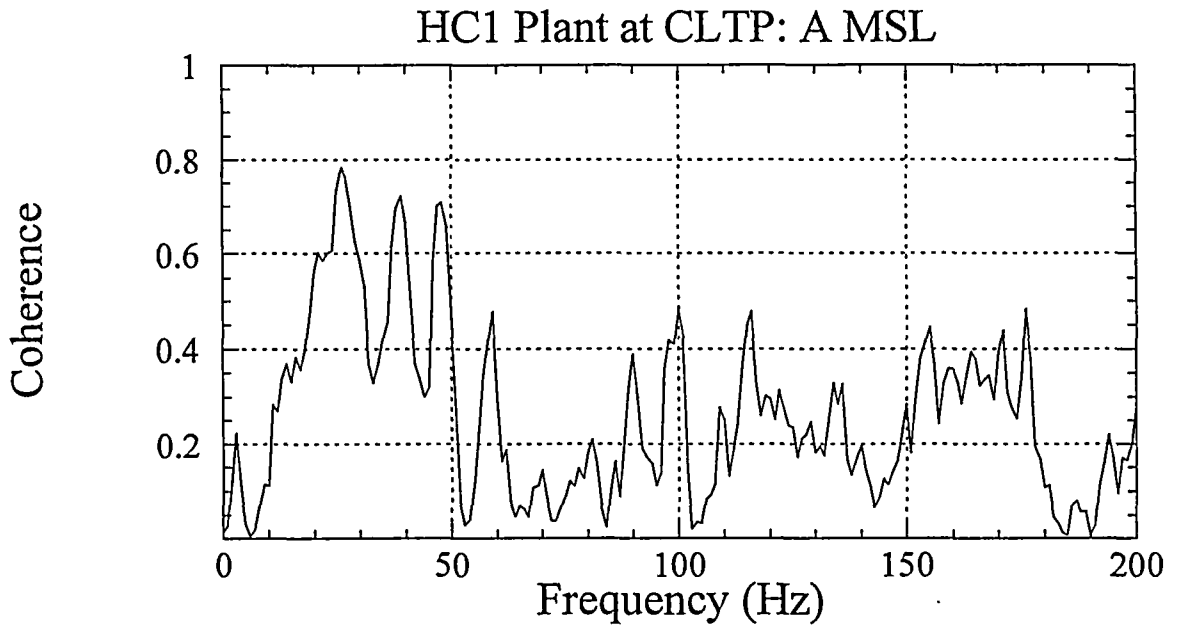

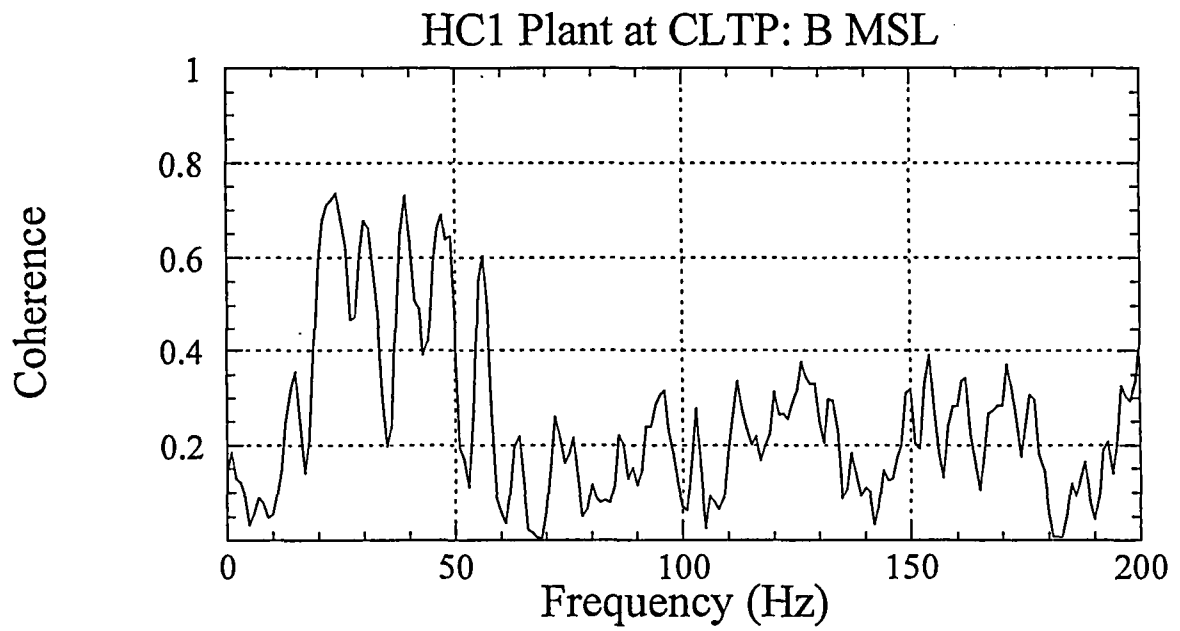

Figure 3.3. Coherence of main steam line (MSL) strain gage data at CLTP power for main steam line A (top) and B (bottom).

Table 3.3. Minimum and maximum pressures, and RMS, in main steam lines A and B in-plant.

Location	Minimum Pressure (psid)	Maximum Pressure (psid)	RMS Pressure (psid)
A Upper	-1.81	1.84	0.47
A Lower	-1.86	1.82	0.43
B Upper	-1.48	1.96	0.42
B Lower	-1.79	1.55	0.40

The load created by substituting the pressure time histories on two main steam lines with pressure time histories on two other main steam lines, then maximizing the load by shifting phase, is expected to be overly conservative. In an effort to quantify this conservatism, an additional calculation was undertaken by making use of data collected on a similar plant (Susquehanna Unit 1) at nearly identical operating conditions.

3.2 In-Plant Conservatism

Recent in-plant strain gage measurements were made at Susquehanna Unit 1 (SQ1) to predict their CLTP dryer loads [4]. All eight strain gages were operational throughout these tests. It is perhaps natural then to ask whether the SQ1 data could be manipulated by substituting main steam line data in a manner similar to what was done for HC1, in an effort to determine the level of conservatism introduced by this approach.

HC1 and SQ1 steam delivery geometries are nearly identical geometrically: their steam dryer geometries are identical (comparing Figure 2.1 in this report with Figure 2.1 in [4]), main steam lines A and D are symmetrical, as are main steam lines B and C, their main steam line diameters are identical (comparing Table 2.1 in this report with the SQ1 data shown in Table 3.4 [4]), and their CLTP conditions are very similar (14.40 Mlbs/hr for HC1, 14.29 Mlbs/hr for SQ1). Their differences include the placement of their strain gages (comparing Table 2.1 with Table 3.4), the differences in locations of their standpipes (comparing Table 3.2 with the SQ1 data shown in Table 3.5 [4]), and the main geometry difference between the two plants, namely the existence of dead-headed branches off main steam lines A and D in SQ1 that are not present in HC1.

Table 3.4. Main steam line lengths at SQ1. The main steam lines are 26 inch Schedule 80 (ID = 23.647 inches).

Main Steam Line	Distance to First Strain Gage (ft)	Distance to Second Strain Gage (ft)
A	22.79	52.67
B	22.79	49.57
C	22.79	48.27
D	22.79	52.58

Table 3.5. Standpipe location summary at SQ1.

Main Steam Line	Distances From Upstream Elbow (ft)
A	Dead-Headed Branch Line
B	3.33, 7.50, and 11.50
C	3.46, 7.63, and 12.86
D	Dead-Headed Branch Line

With these differences the two plants cannot entirely replicate each other. However, the intent here is to note their similarities, manipulate the SQ1 data to determine the level of conservatism built into the assumption of replacing the data on two main steam lines (by comparing with and without this substitution), and then argue that the same level of conservatism is consistent between plants.

Symmetry between the loads on main steam lines A and D, and B and C, at SQ1, may be seen in Figures 3.4 and 3.5, comparing the PSDs of these signals at CLTP conditions. Note the 15 Hz signal seen in main steam lines A and D.

The maximum loads on the dryer were found by replacing the A and B main steam line SQ1 data with the D and C main steam line data, respectively, then adjusting the phase of the time signals on the A and B main steam line strain gage data in a fashion identical to what was undertaken when computing the CLTP load with the HC1 data. This step was accomplished by repeatedly dropping time step information from main steam line A, then from main steam line B, then back to main steam line A for confirmation, until the maximum load on the dryer was achieved. This maximum low resolution load was then used to establish the number of time steps to drop from the C signal (now the B signal) and the D signal (now the A signal) to represent the replaced signals.

3.3 Subscale Data

A subscale test was conducted on a 1/8th scale representation of the HC1 steam delivery system. This work, detailed in [5], conservatively predicted the CLTP and Extended Power Uprate (EPU) loads to be anticipated on the HC1 steam dryer. These subscale loads were corrected back to full scale by correcting the frequency of data collection (reducing the frequency by a factor of 5.686) and the pressure magnitude (multiplying the pressure by a factor of 5.164) on the eight pressure transducers on the four main steam lines. Figures 3.6 to 3.13 present the PSDs of these eight transducers at the CLTP and EPU power levels. The pressure levels are summarized in Table 3.6. It may be seen that the CLTP RMS pressure values from subscale, corrected back to full scale, are on average double the CLTP RMS pressure values from the in-plant data. In addition, the EPU RMS pressure values from subscale, corrected back to full scale, are on average 37% larger than the CLTP RMS pressure values from subscale, also corrected back to full scale.

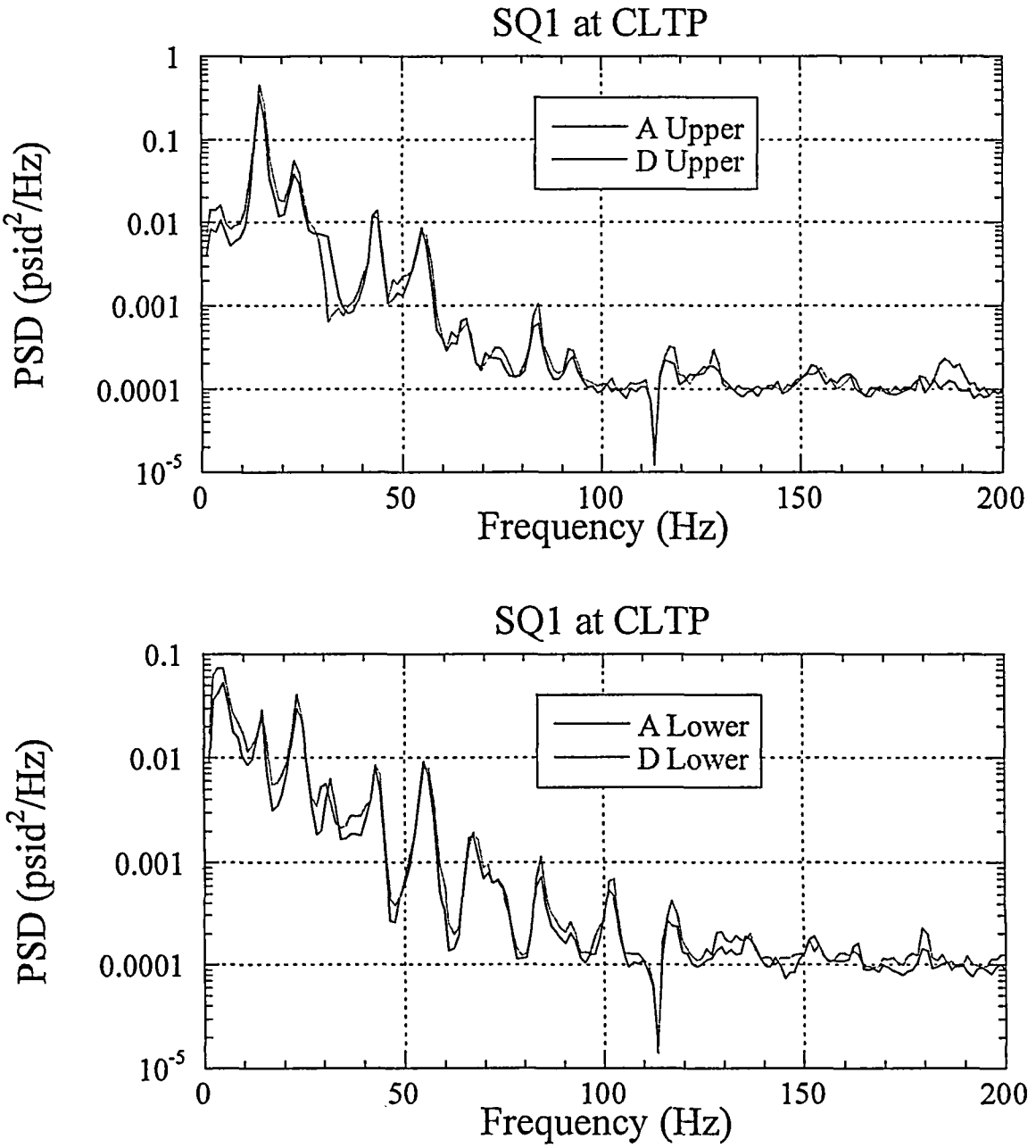

Figure 3.4. PSD comparison of pressure transducer data at CLTP, for main steam line A and D at SQ1: upstream location (top), downstream location (bottom).

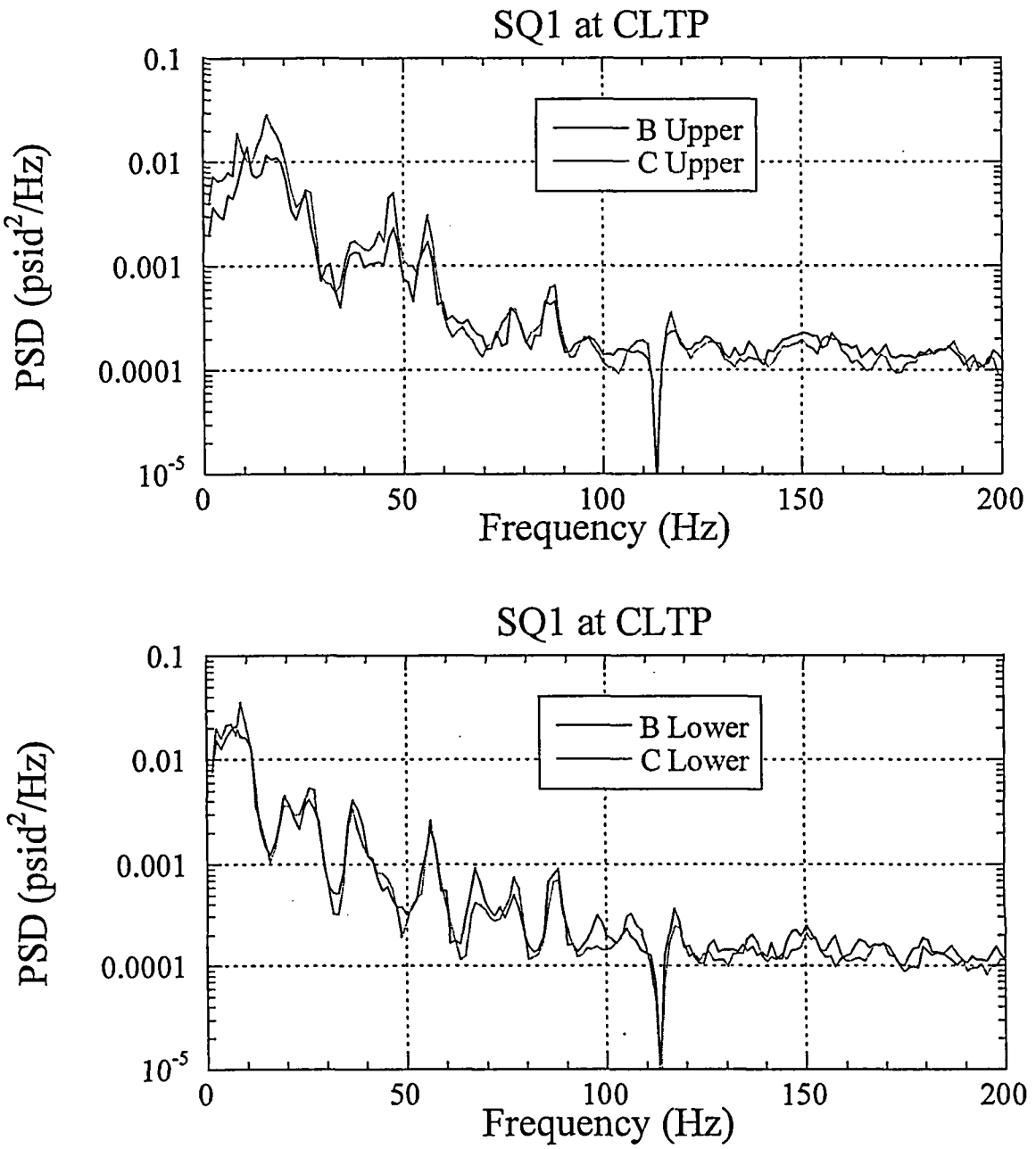

Figure 3.5. PSD comparison of pressure transducer data at CLTP, for main steam line B and C at SQ1: upstream location (top), downstream location (bottom).

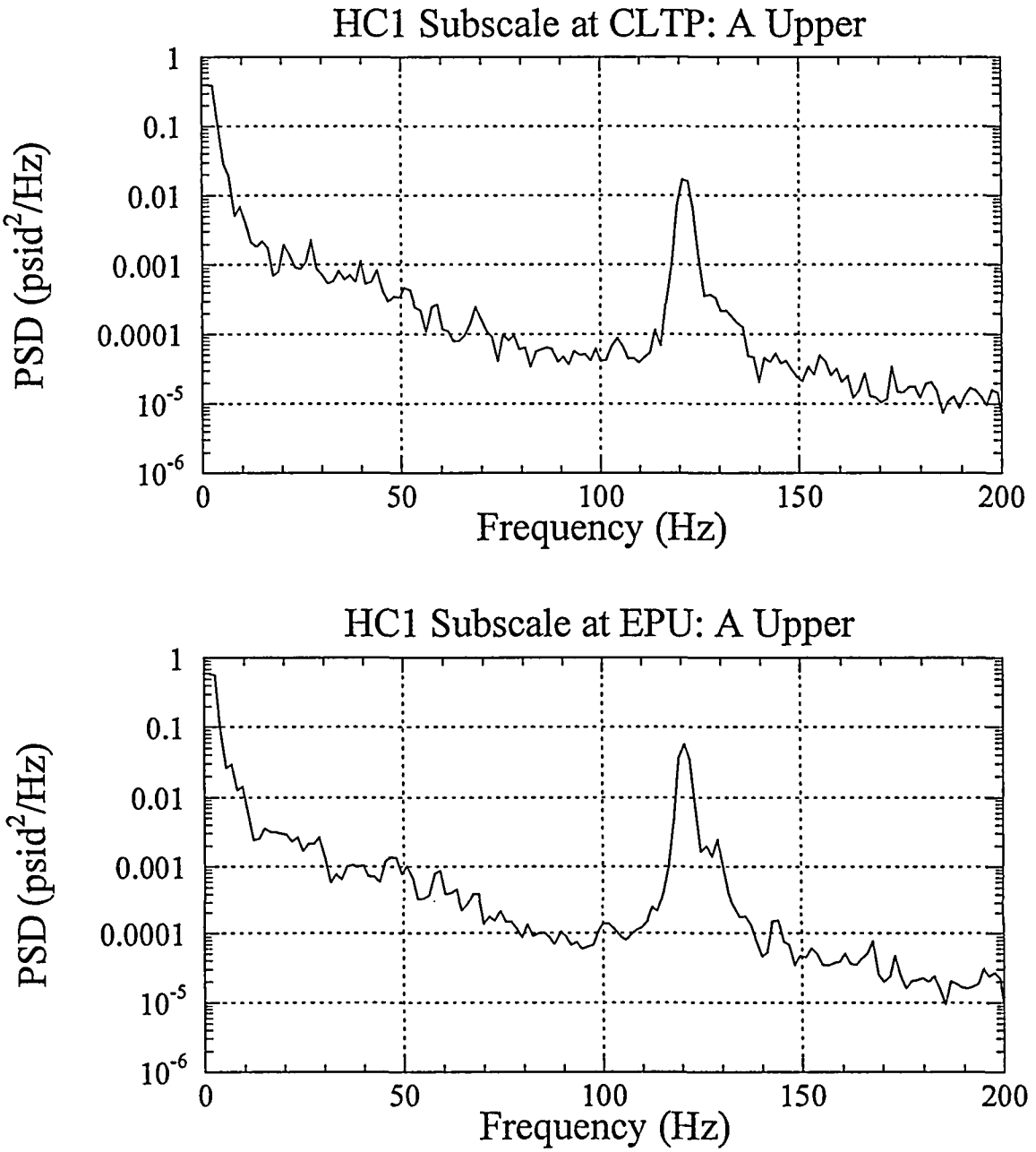

Figure 3.6. PSD comparison of pressure transducer data at CLTP (top) and EPU (bottom), for main steam line A, upstream location.

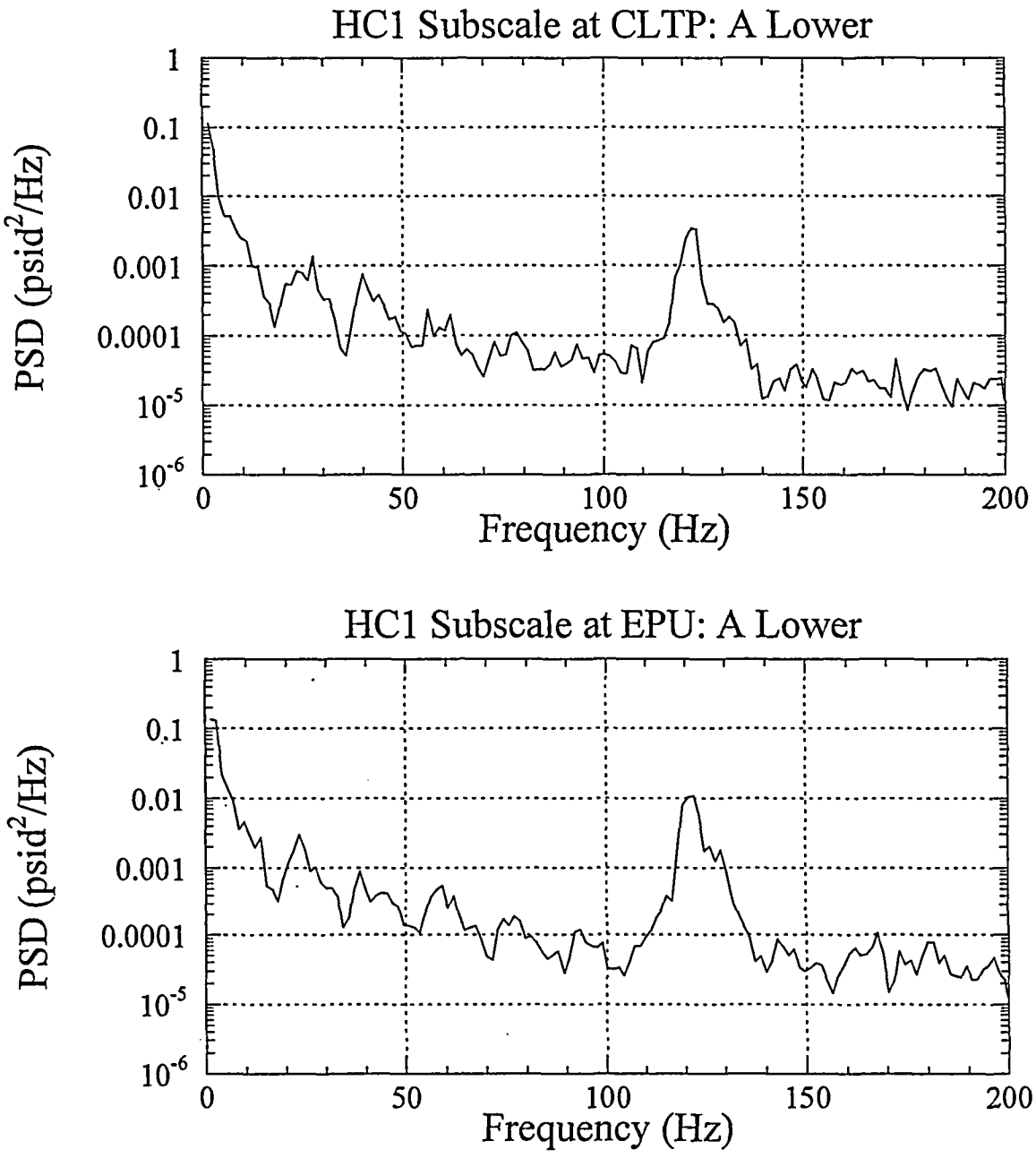

Figure 3.7. PSD comparison of pressure transducer data at CLTP (top) and EPU (bottom), for main steam line A, downstream location.

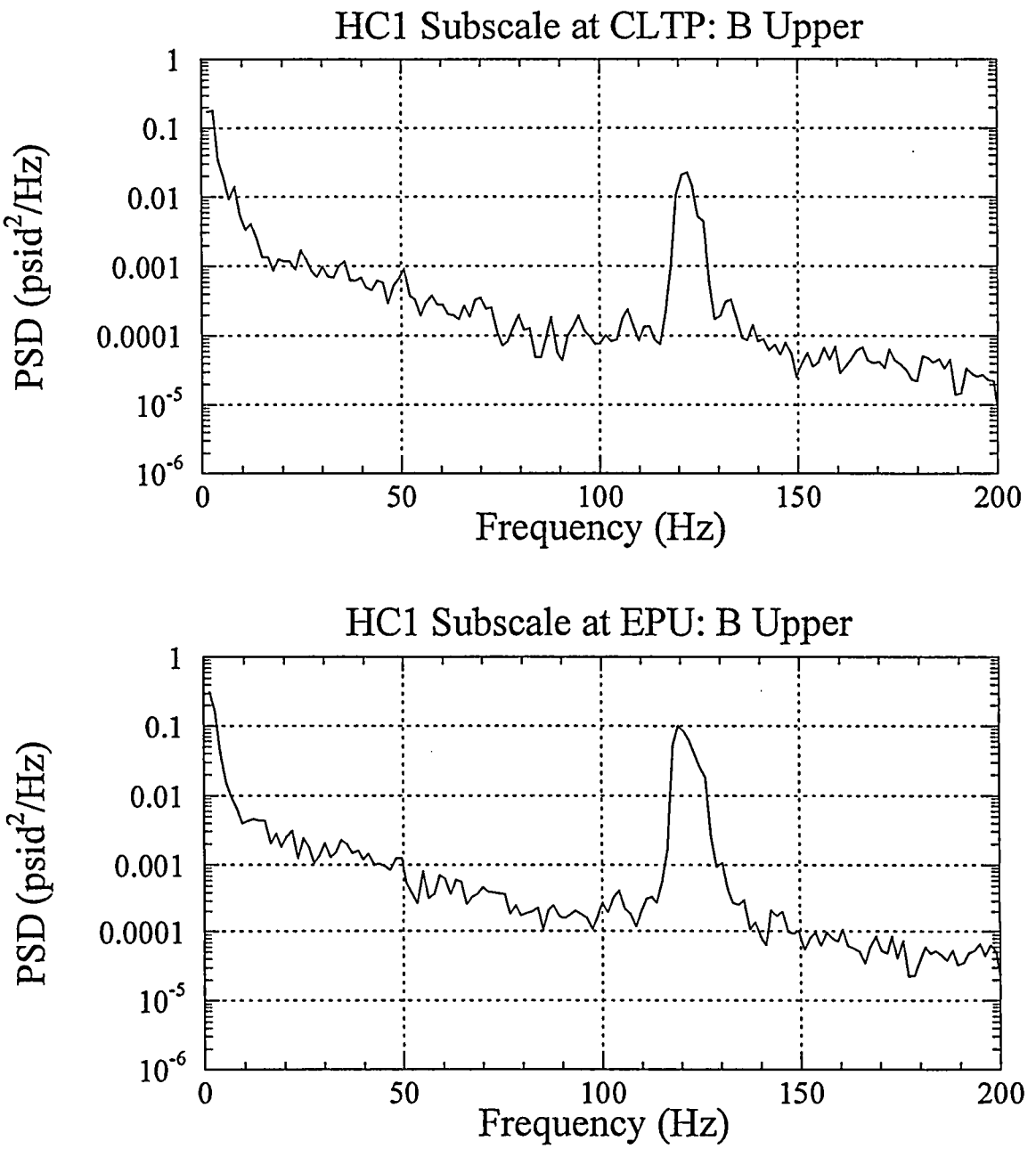

Figure 3.8. PSD comparison of pressure transducer data at CLTP (top) and EPU (bottom), for main steam line B, upstream location.

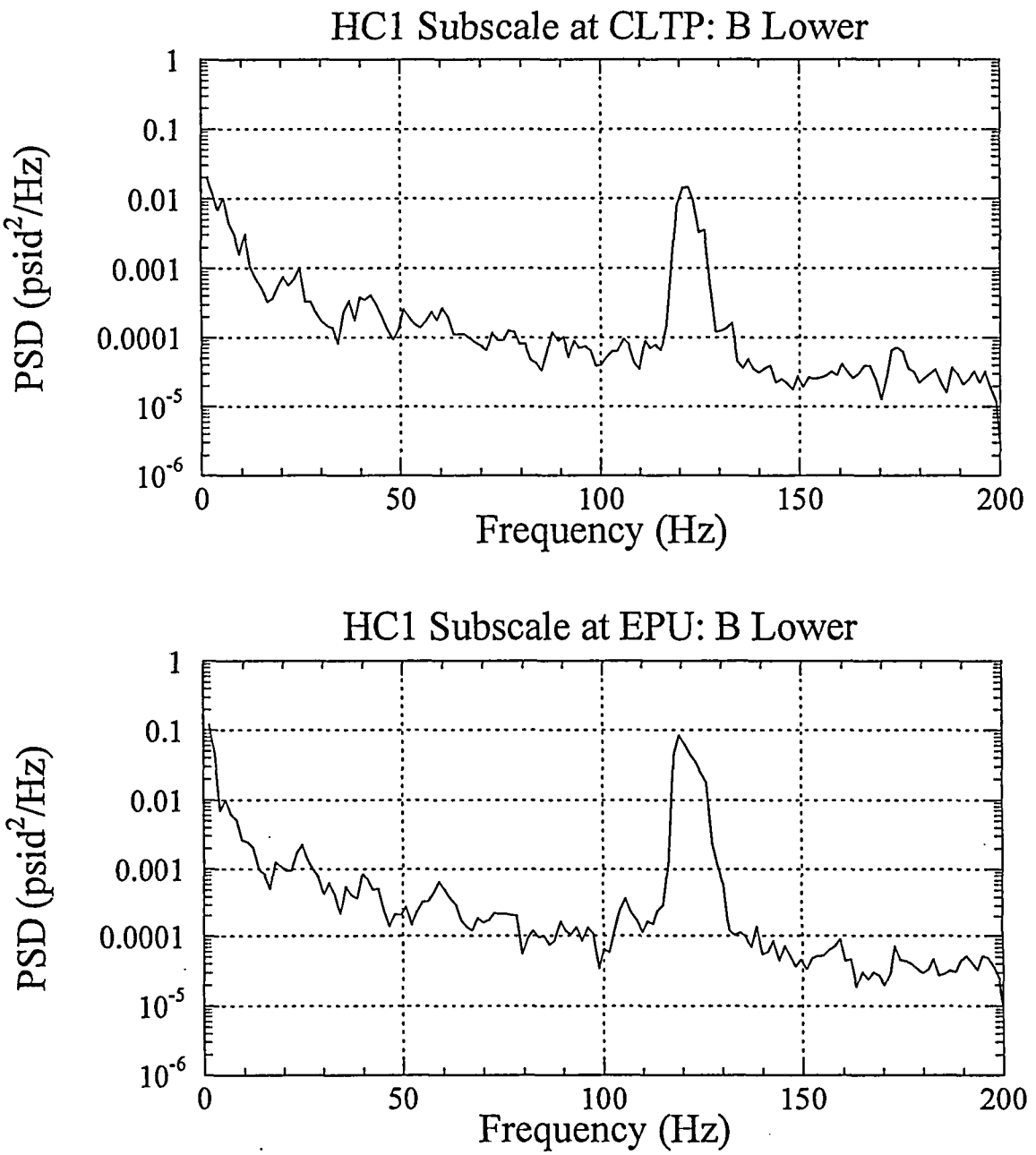

Figure 3.9. PSD comparison of pressure transducer data at CLTP (top) and EPU (bottom), for main steam line B, downstream location.

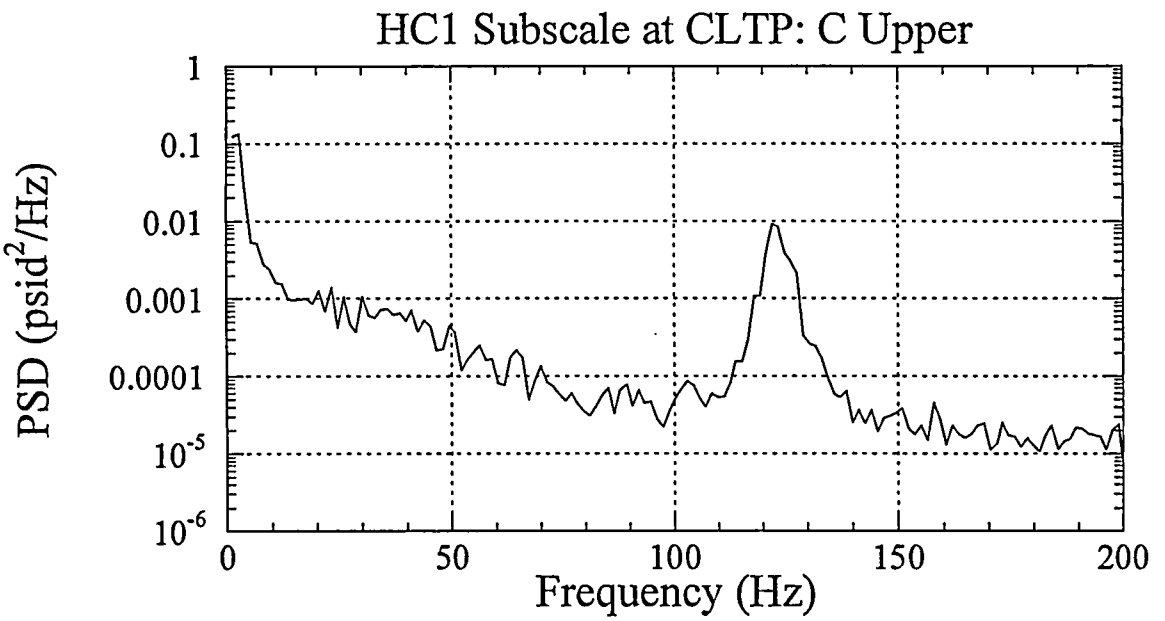

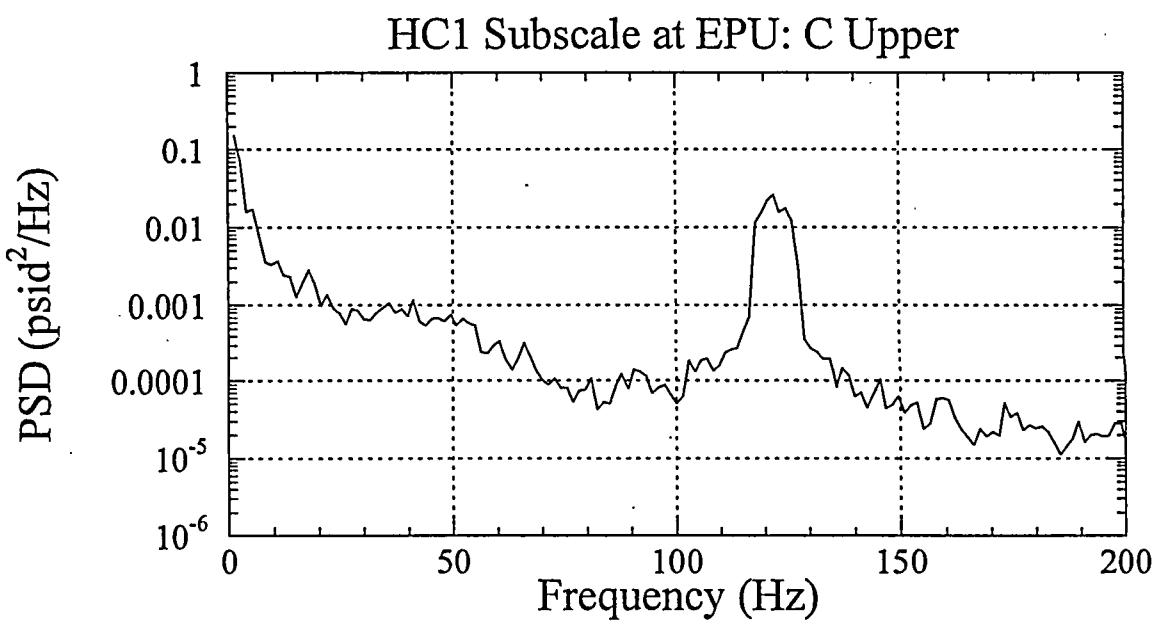

Figure 3.10. PSD comparison of pressure transducer data at CLTP (top) and EPU (bottom), for main steam line C, upstream location.

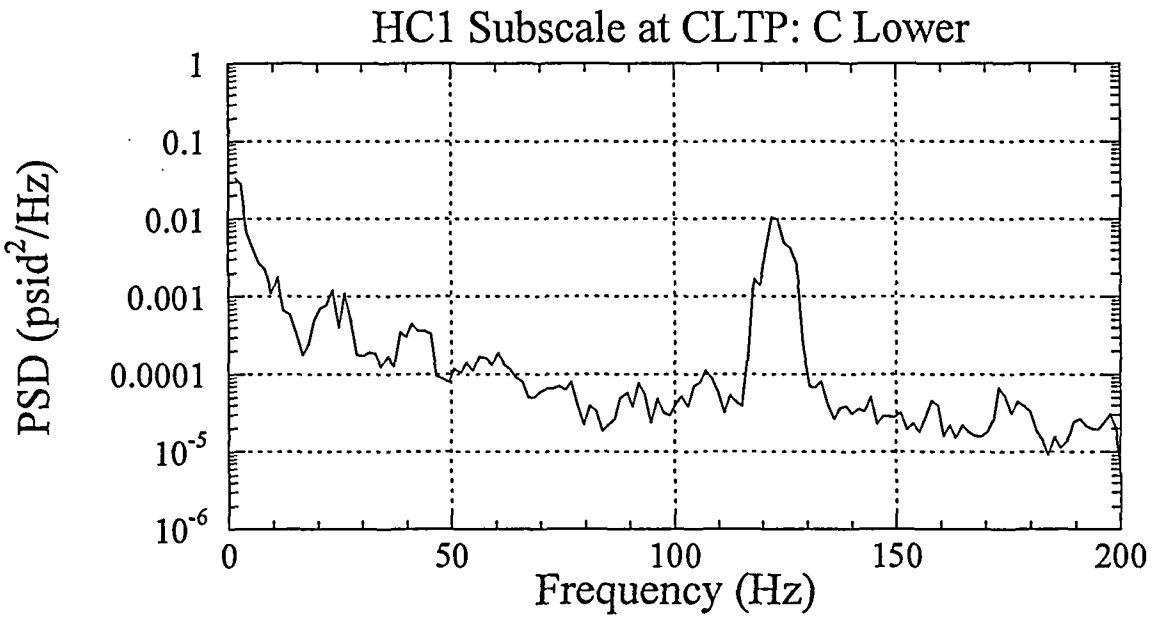

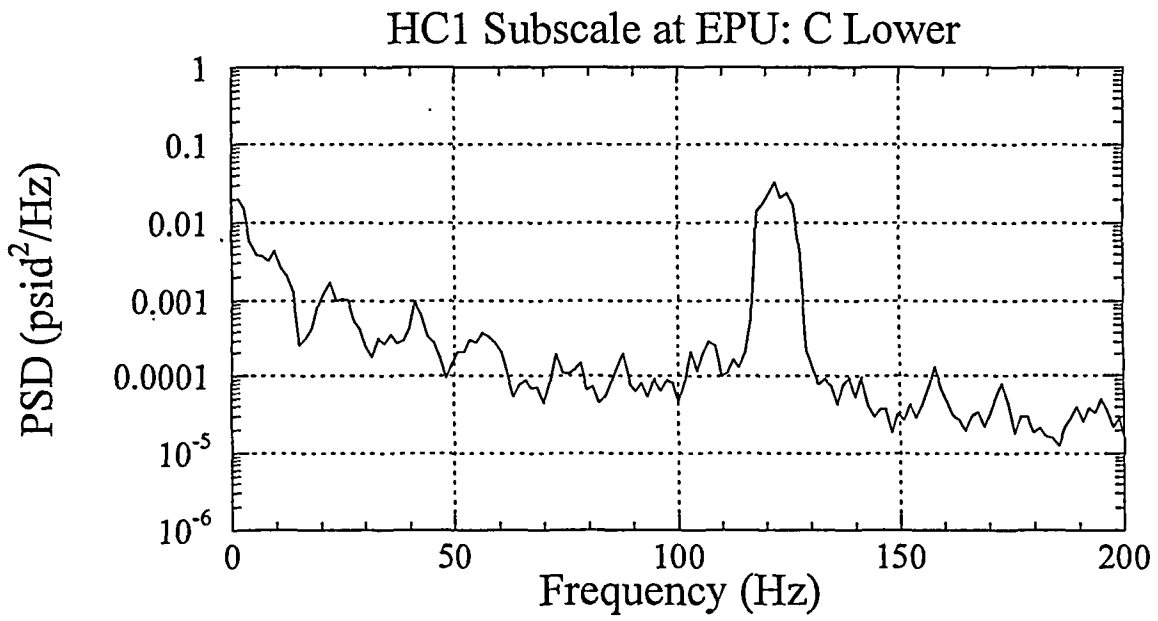

Figure 3.11. PSD comparison of pressure transducer data at CLTP (top) and EPU (bottom), for main steam line C, downstream location.

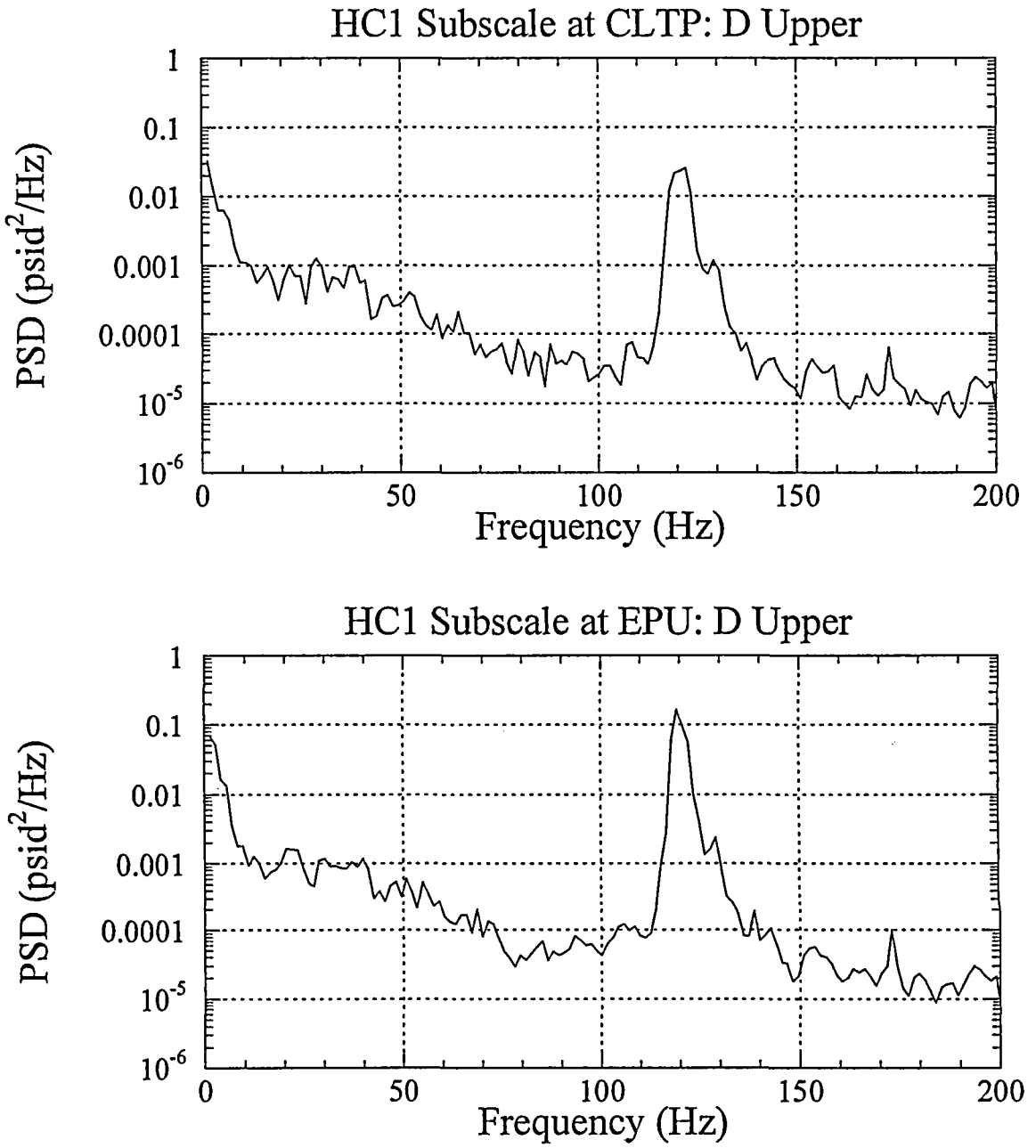

Figure 3.12. PSD comparison of pressure transducer data at CLTP (top) and EPU (bottom), for main steam line D, upstream location.

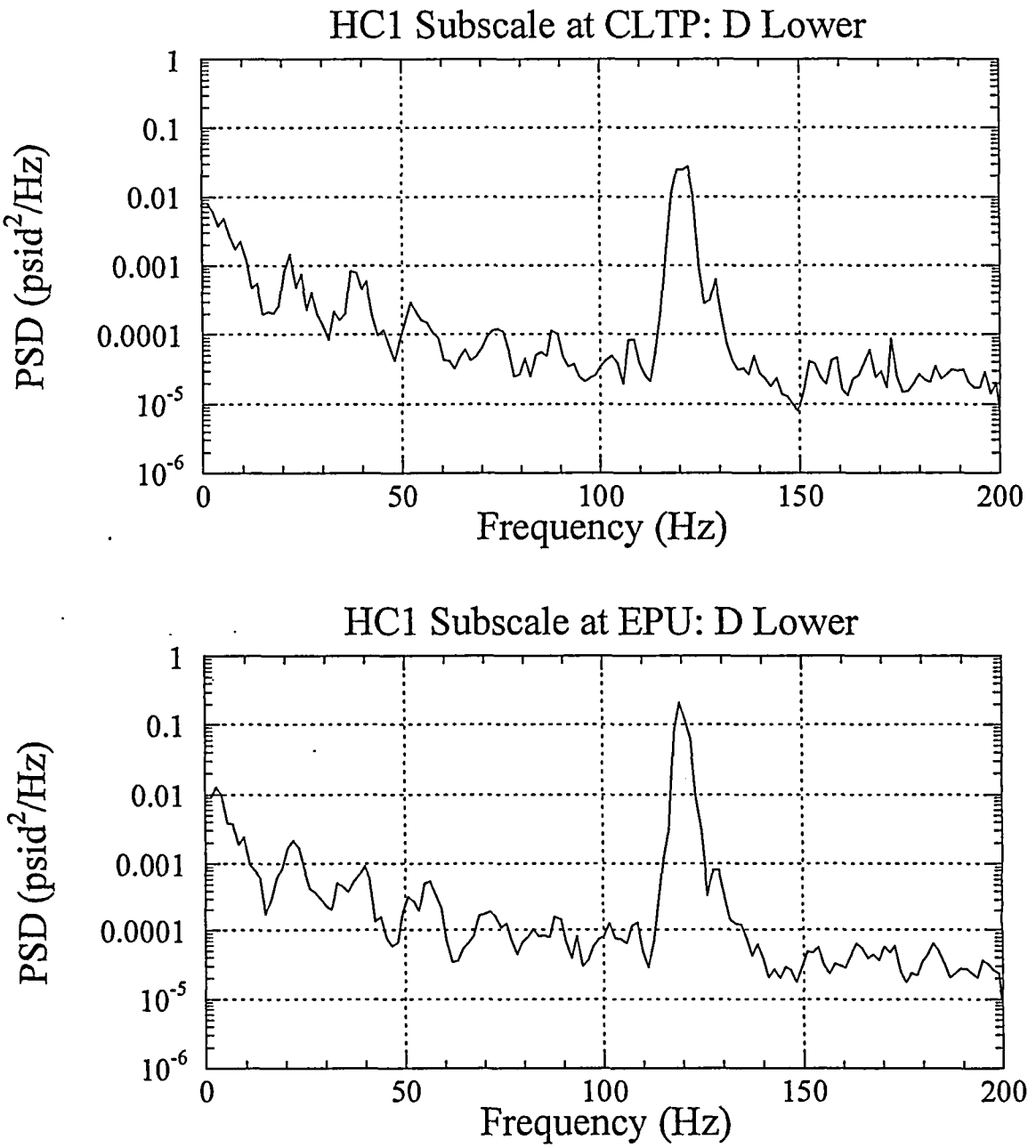

Figure 3.13. PSD comparison of pressure transducer data at CLTP (top) and EPU (bottom), for main steam line D, downstream location.

Table 3.6. Minimum and maximum pressures, and RMS, in the four main steam lines for the subscale tests at the conditions shown.

CLTP Power Level

Location	Minimum Pressure (psid)	Maximum Pressure (psid)	RMS Pressure (psid)
A Upper	-6.45	7.25	2.03
A Lower	-3.47	2.15	0.76
B Upper	-3.94	3.61	1.19
B Lower	-3.73	1.79	0.68
C Upper	-4.09	2.58	1.02
C Lower	-2.08	2.01	0.63
D Upper	-3.13	2.66	0.93
D Lower	-2.05	1.73	0.60

EPU Power Level

Location	Minimum Pressure (psid)	Maximum Pressure (psid)	RMS Pressure (psid)
A Upper	-7.27	5.92	2.23
A Lower	-3.35	3.05	0.96
B Upper	-5.99	4.31	1.44
B Lower	-4.53	2.83	1.14
C Upper	-3.43	2.74	1.08
C Lower	-3.02	2.26	0.84
D Upper	-3.55	2.74	1.16
D Lower	-2.61	2.18	0.98

4. Results

The main steam line pressure data were used to drive the verified acoustic circuit model for the HC1 steam dome and main steam lines. Results are presented on a low-resolution grid (shown schematically in Figures 4.1 to 4.4) by summarizing the peak and RMS pressures expected over the time interval provided in the original data. High resolution loads were subsequently computed, for evaluation by a finite element model of the HC1 dryer.

4.1 In-Plant CLTP

Nodal results are shown in Figure 4.5 for the CLTP power level. A non-physical 80 Hz signal has been removed from the in-plant predictions [6].

Comparisons may be further made at the center edge of the cover plates with the outer bank hoods, on either side of the dryer, at nodes 7 and 99 (as located in Figures 4.1 and 4.3). Pressure time-history and PSD plots are shown in Figure 4.6.

4.2 In-Plant Conservatism

Results of the main steam line substitution for SQ1 data, as discussed previously in Section 3.2, found that the maximum pressure difference on the dryer increases from 0.302 psid (with all eight strain gages active) to 0.404 (with the substitution and modification of two main steam lines), an increase of 33% (a comparable result was found when using subscale data [7]). This conservatism then suggests that the pressure levels shown in Figures 4.5 and 4.6 should be multiplied by 0.75, whereas the PSD levels should be multiplied by 0.56, to remove conservatism built into the predictions when main steam line data are replaced and modified. The resulting peak loads are shown in Figure 4.7. Rev 2

4.3 Subscale CLTP and EPU

Nodal results are shown in Figure 4.8 for the CLTP and EPU power levels extracted from the 1/8th scale tests. A non-physical 80 Hz signal has been removed from the in-plant predictions [6]. It may be seen that the peak differential pressure from the in-plant CLTP prediction is 0.18 psid, while the peak differential pressure from the subscale CLTP, corrected to full scale, is 0.76, an increase of over a factor of 4. Also, the peak differential pressure from the subscale EPU, corrected to full scale, is 1.19, an increase of 57% over the corrected subscale CLTP value, consistent with the RMS pressure increase recorded in the subscale main steam lines.

Comparisons may be further made at the center edge of the cover plates with the outer bank hoods, on either side of the dryer, at nodes 7 and 99 (as located in Figures 4.1 and 4.3). Pressure time-history and PSD plots are shown in Figures 4.9 and 4.10.

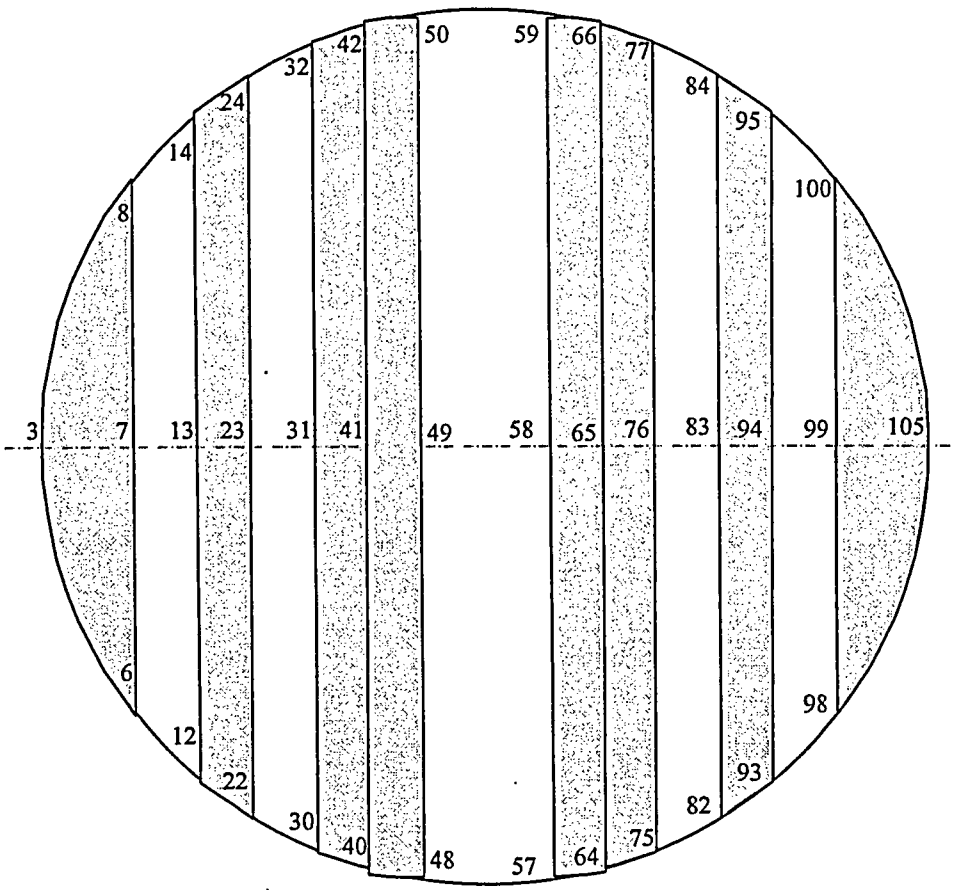

Figure 4.1. Bottom plates pressure node locations, with pressures acting downward in the notation defined here.

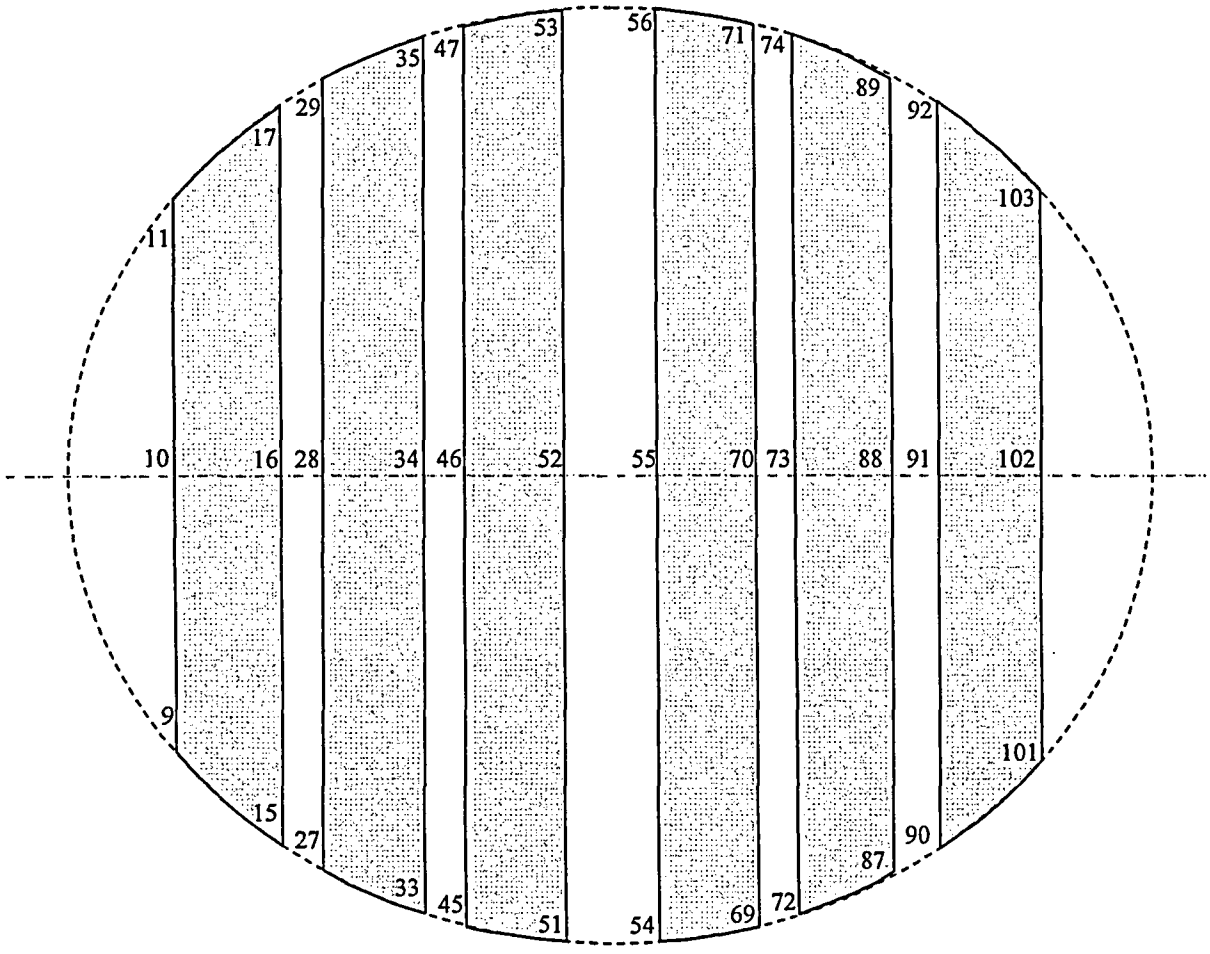

Figure 4.2. Upper plates pressure node locations, with pressures acting downward in the notation defined here.

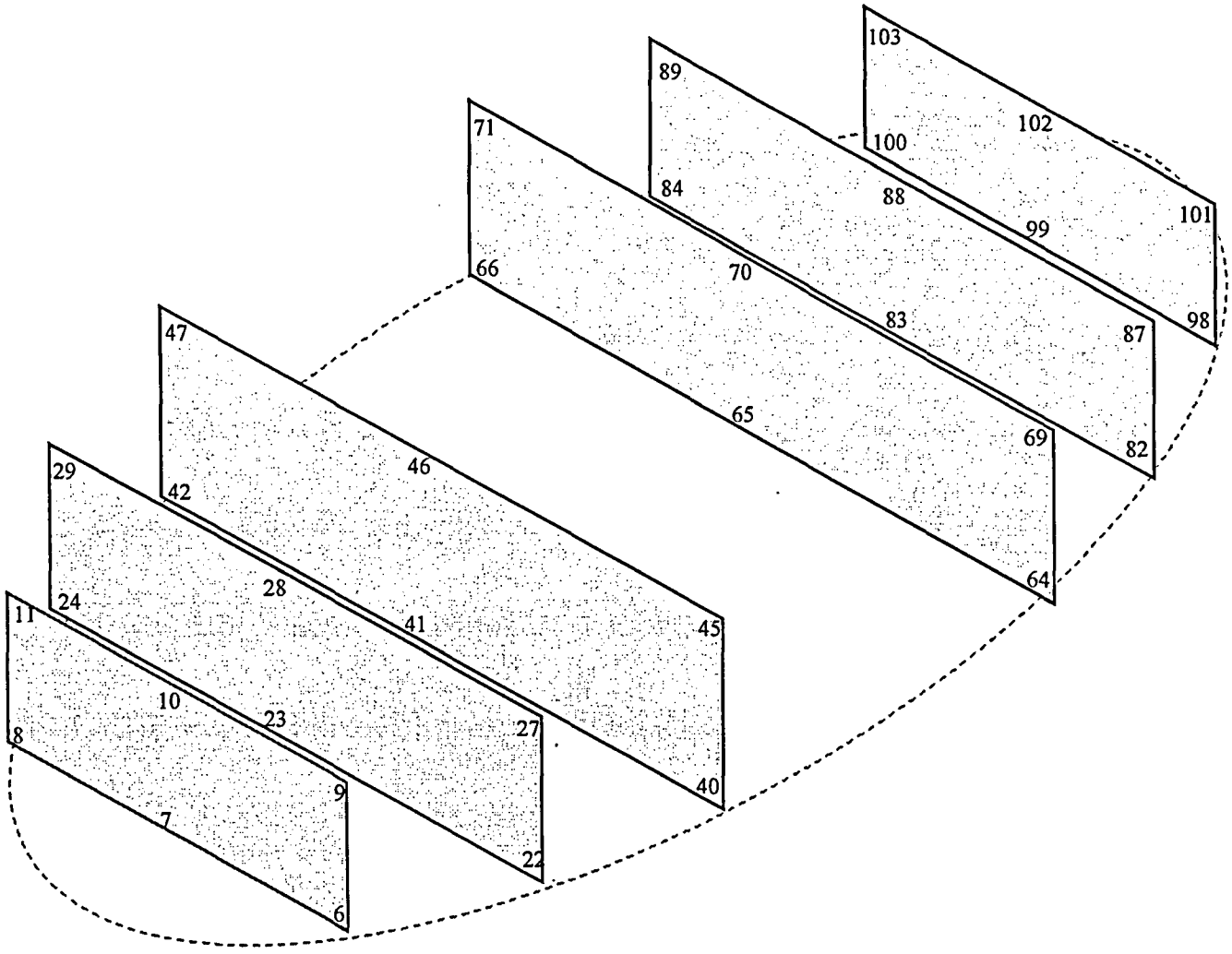

Figure 4.3. Vertical plates: Pressures acting left to right on panels 6-11, 22-29, and 40-47; acting right to left on panels 64-71, 82-89, and 98-103.

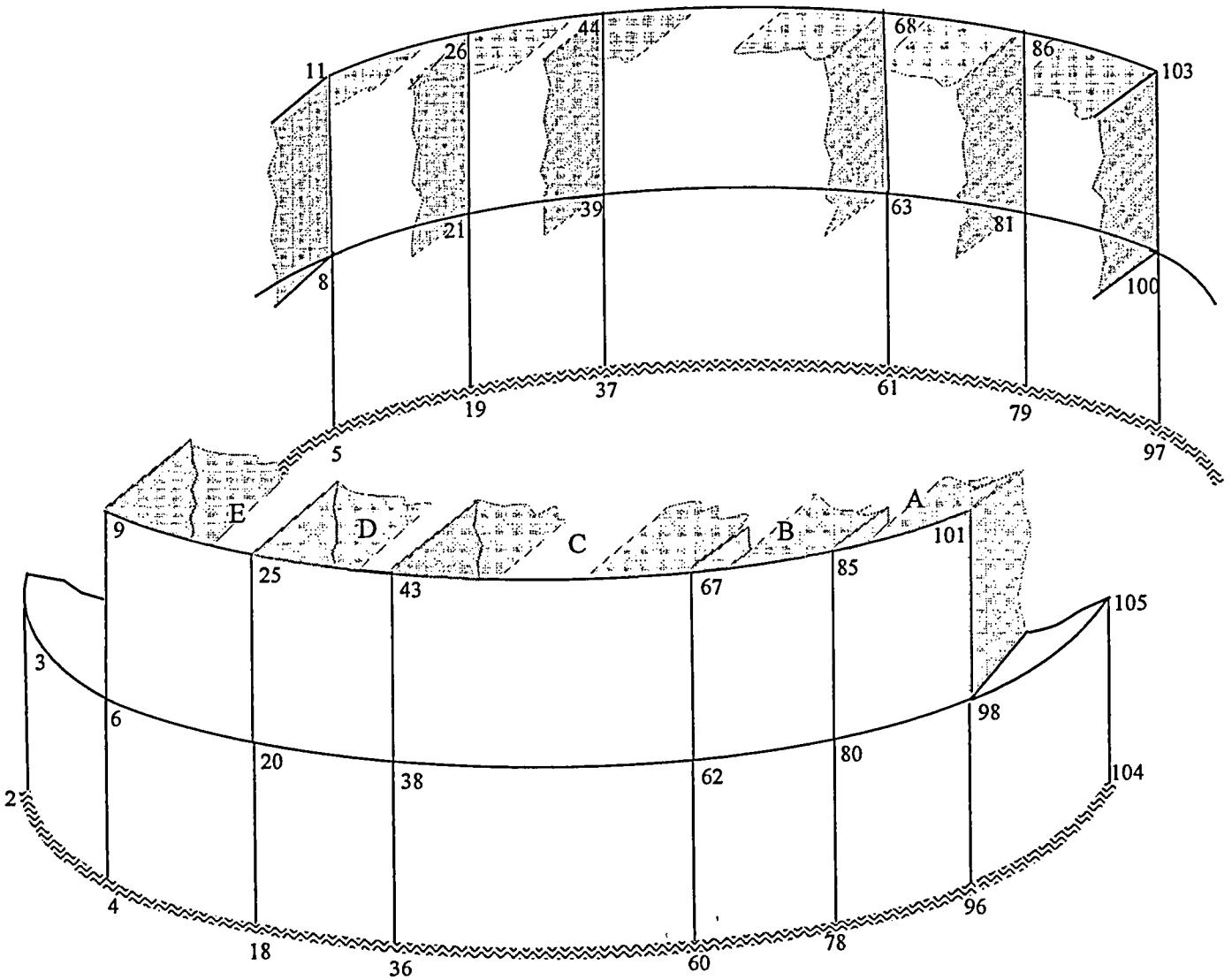

Figure 4.4. Skirt plates: Pressure acting on the outer dryer 0/180 surfaces and the skirt.

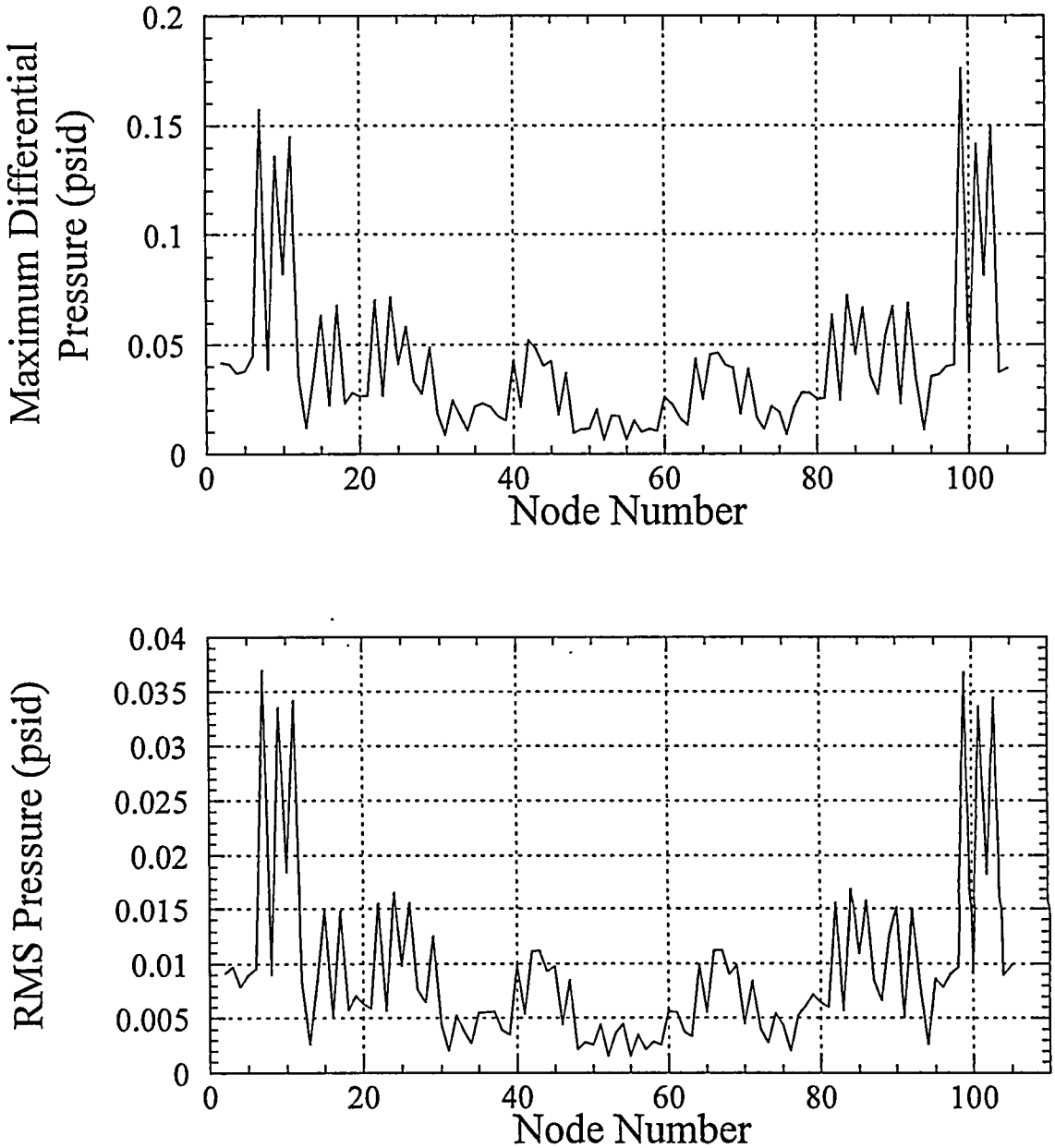

Figure 4.5. Predicted loads at CLTP power level as developed by the current methodology to 200 Hz. Node 7 is located at the back center edge of the cover plate opposite the C and D main steam lines, while node 99 is located at the back center edge of the cover plate opposite the A and B main steam lines.

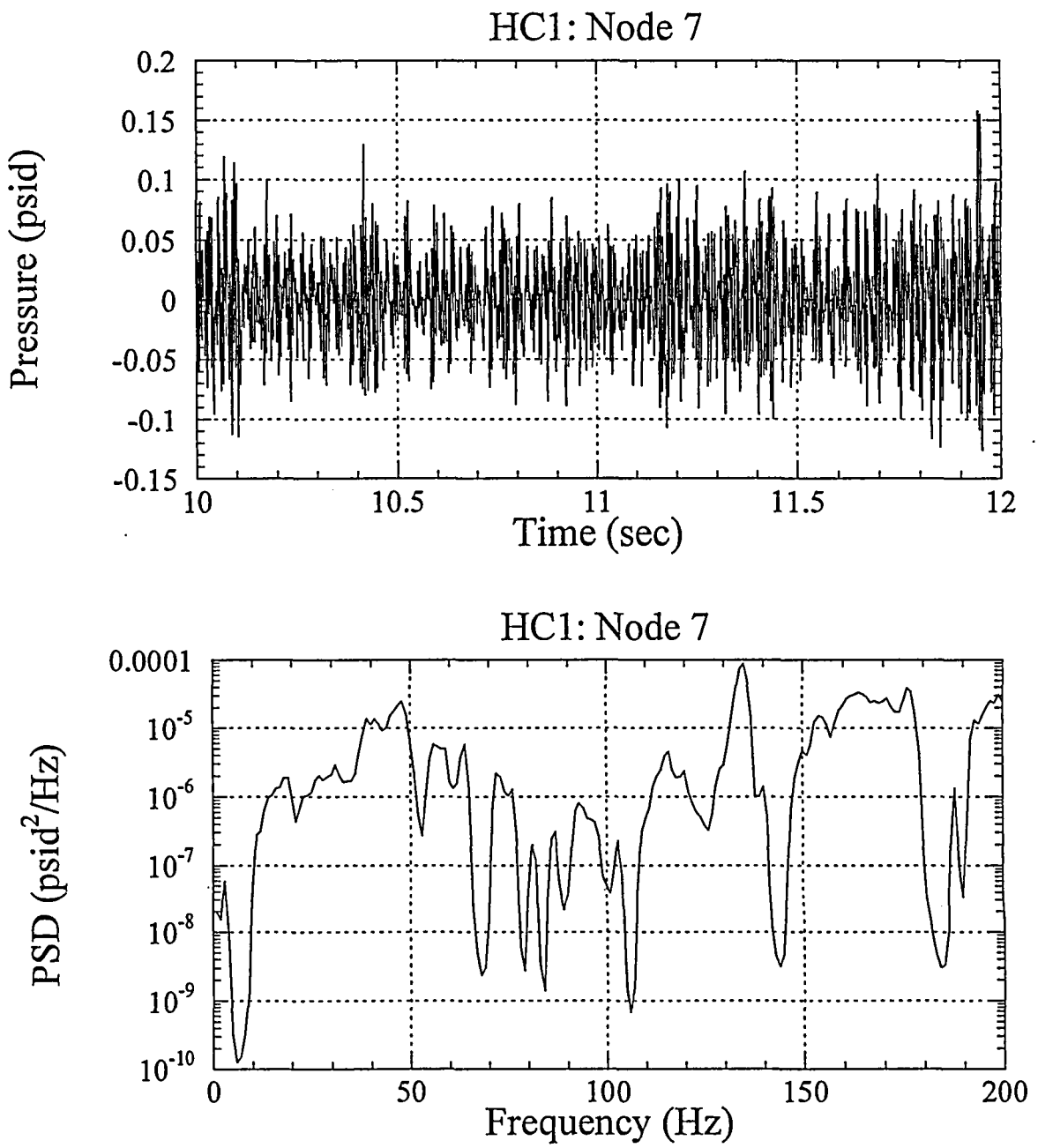

Figure 4.6. Time history and PSD of the predicted CLTP pressure load at the center edge of the cover plate with the outer bank hood for node 7 opposite the C-D side of the dryer.

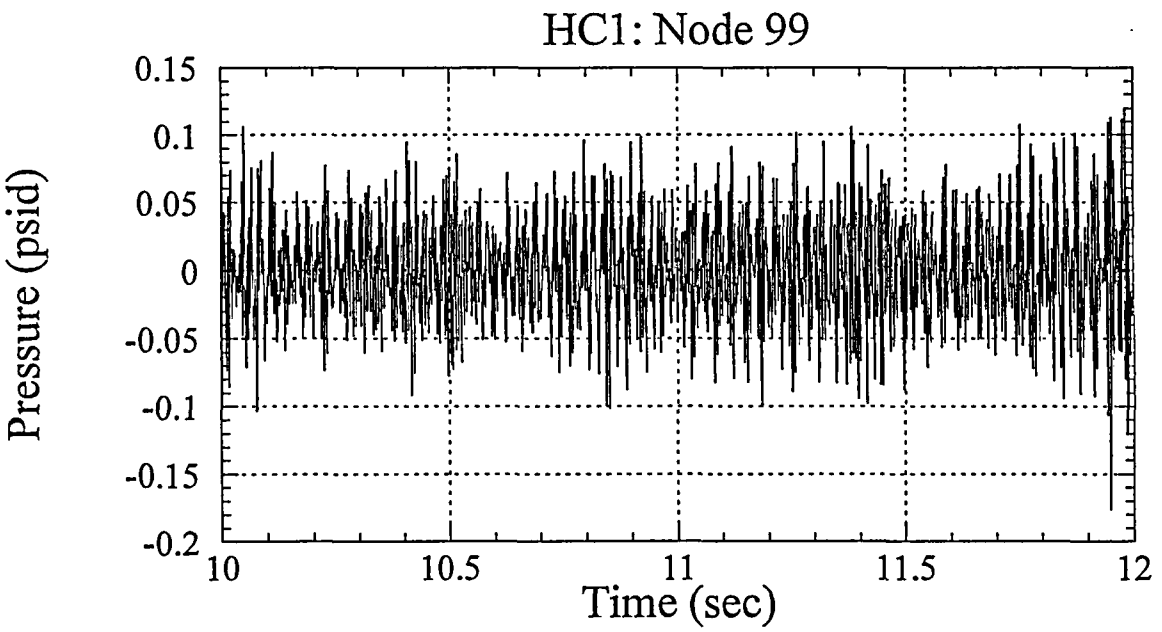

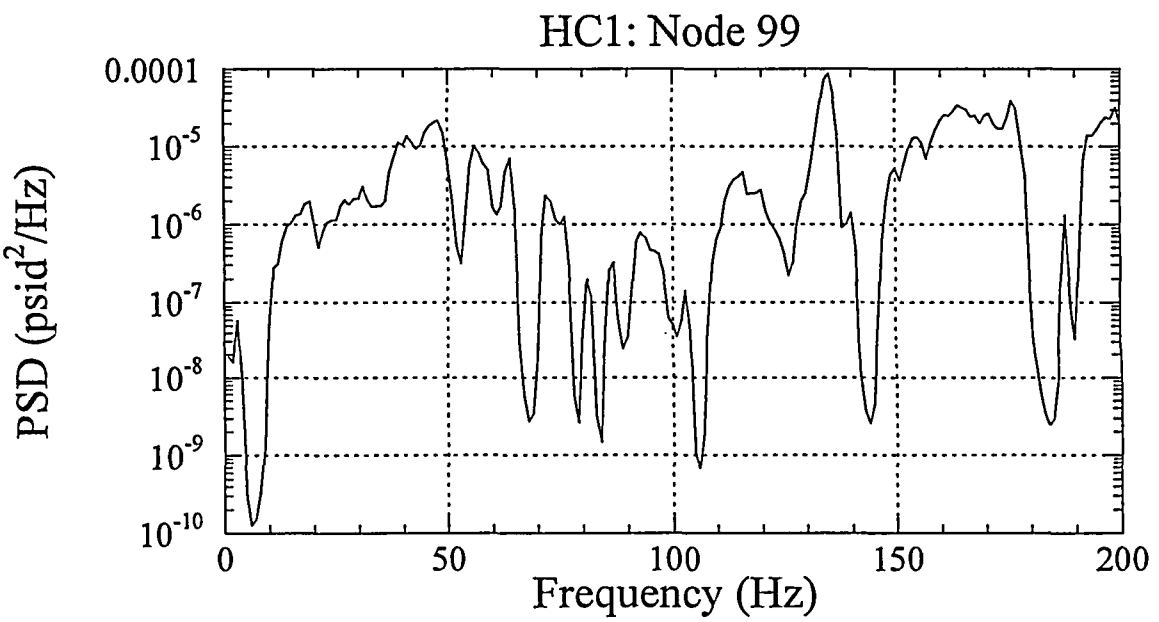

Figure 4.6 (continued). Time history and PSD of the predicted CLTP pressure load at the center edge of the cover plate with the outer bank hood for node 99 opposite the A-B side of the dryer.

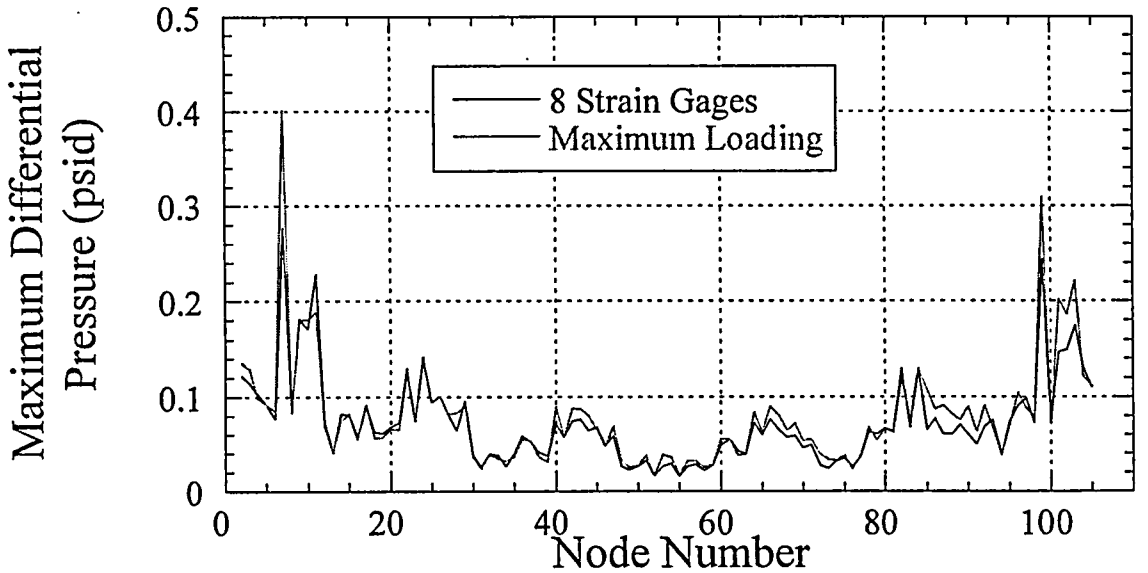

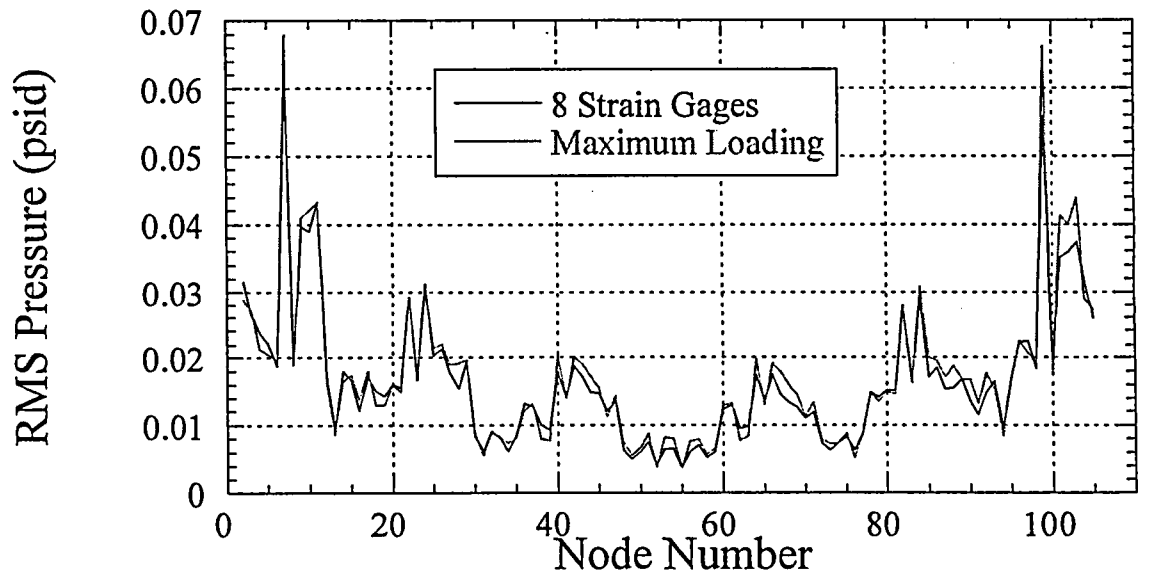

Figure 4.7. Predicted loads at CLTP for SQ1, as developed by the current methodology to 250 Hz. The curves compare the inclusion of all eight strain gage readings (8 Strain Gages) and the substitution of main steam lines A and B with main steam lines D and C, respectively, and the shifting of the time histories to maximize the pressure loading on the dryer (Maximum Loading).

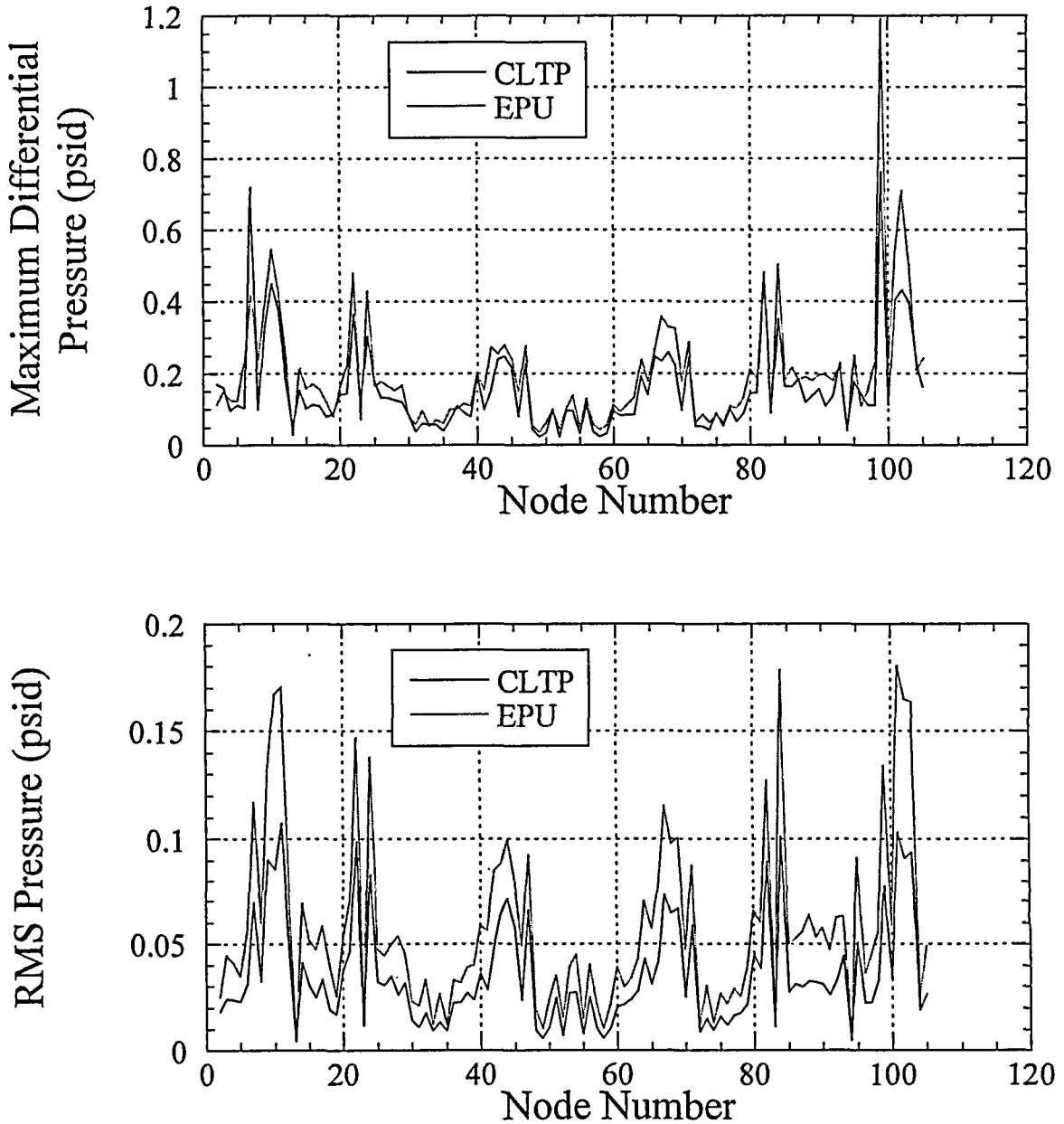

Figure 4.8. Predicted loads at CLTP and EPU power levels as developed by the current methodology to 200 Hz, based on subscale test results. Node 7 is located at the back center edge of the cover plate opposite the C and D main steam lines, while node 99 is located at the back center edge of the cover plate opposite the A and B main steam lines.

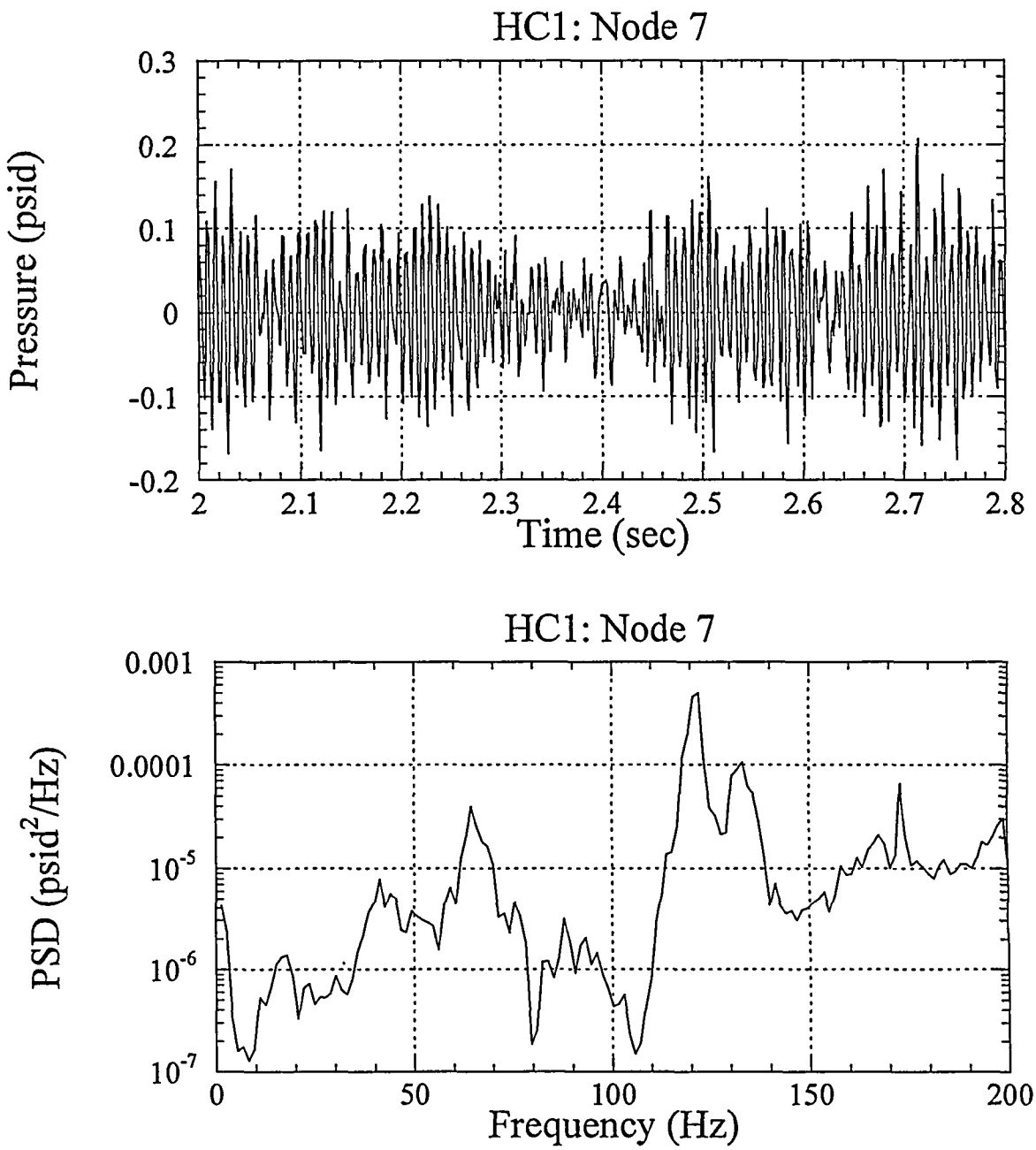

Figure 4.9. Time history and PSD of the predicted CLTP pressure load (extracted from subscale tests) at the center edge of the cover plate with the outer bank hood for node 7 opposite the C-D side of the dryer.

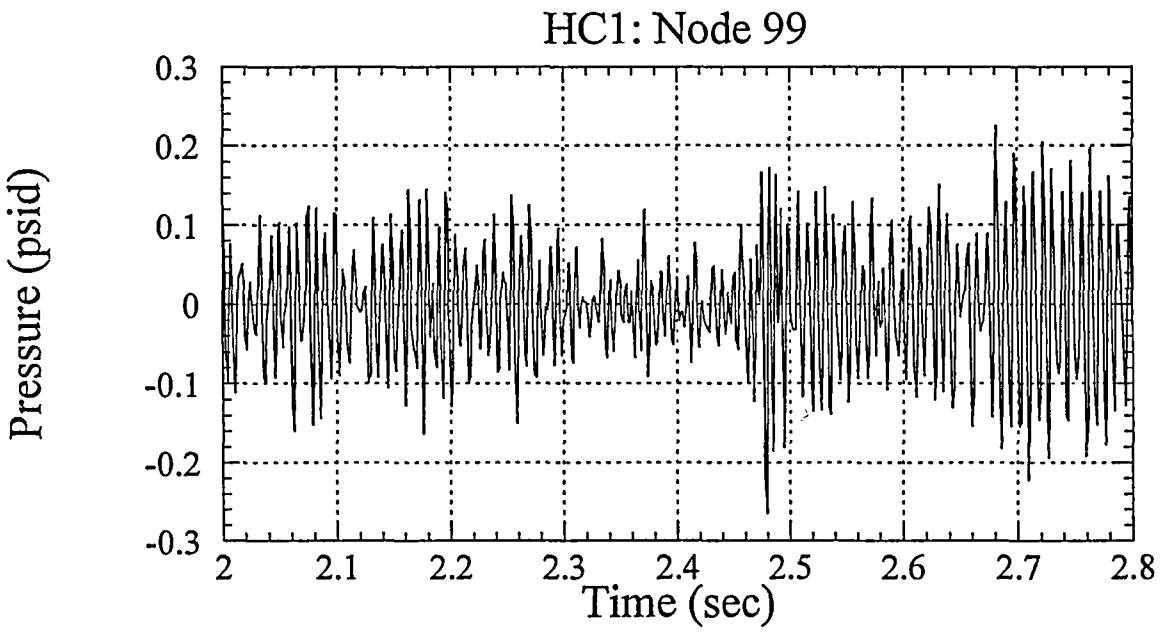

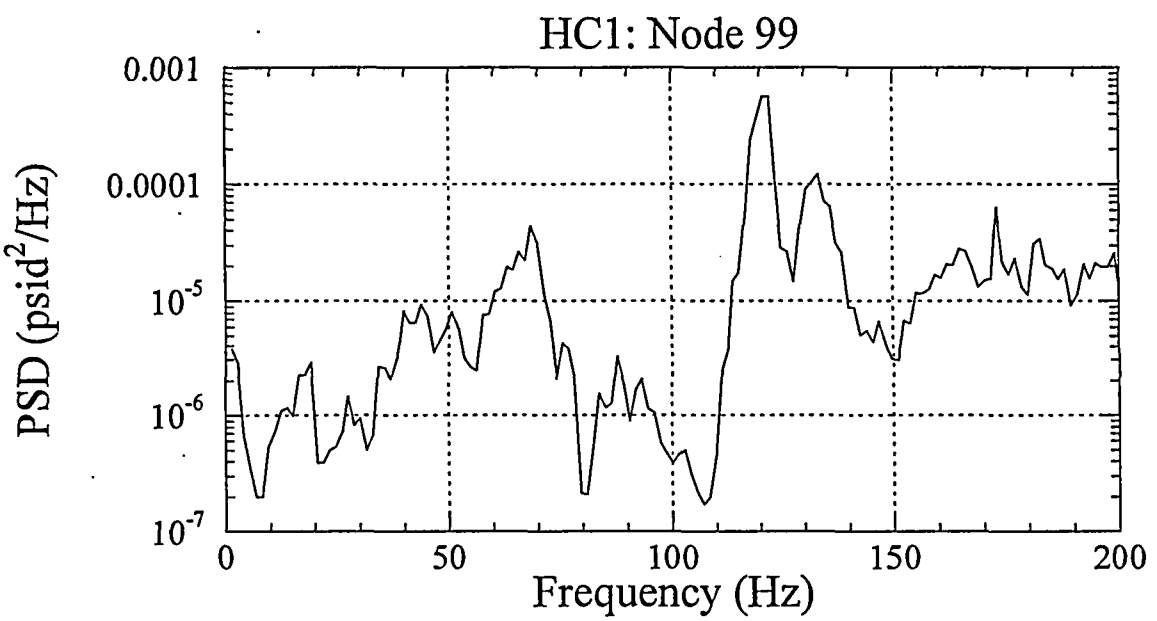

Figure 4.9 (continued). Time history and PSD of the predicted CLTP pressure load (extracted from subscale test results) at the center edge of the cover plate with the outer bank hood for node 99 opposite the A-B side of the dryer.

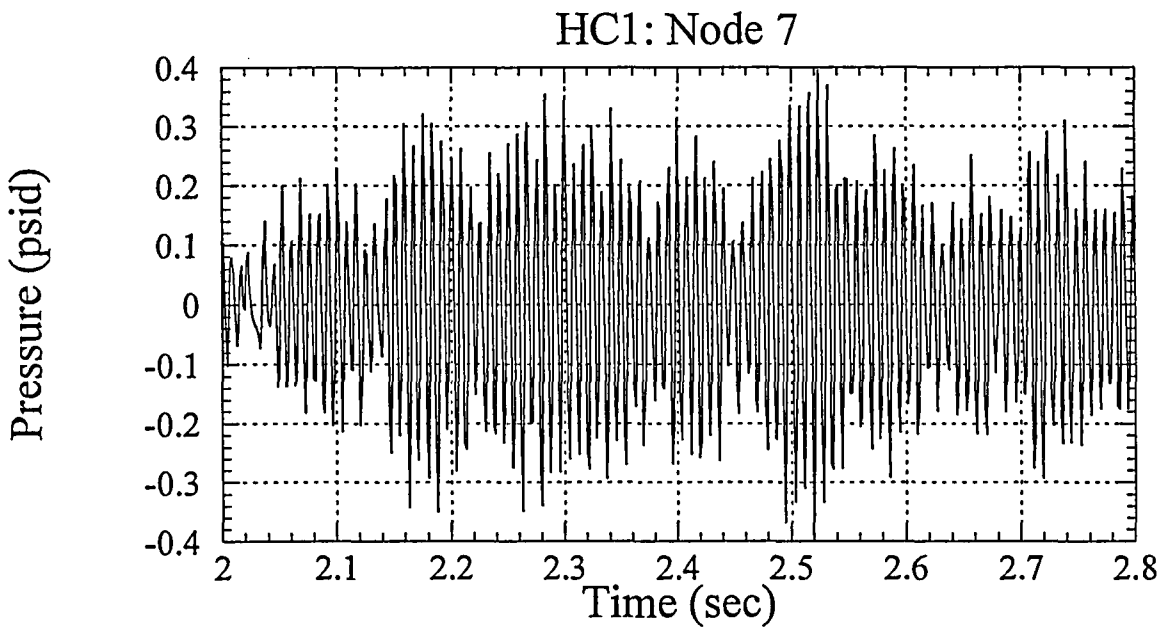

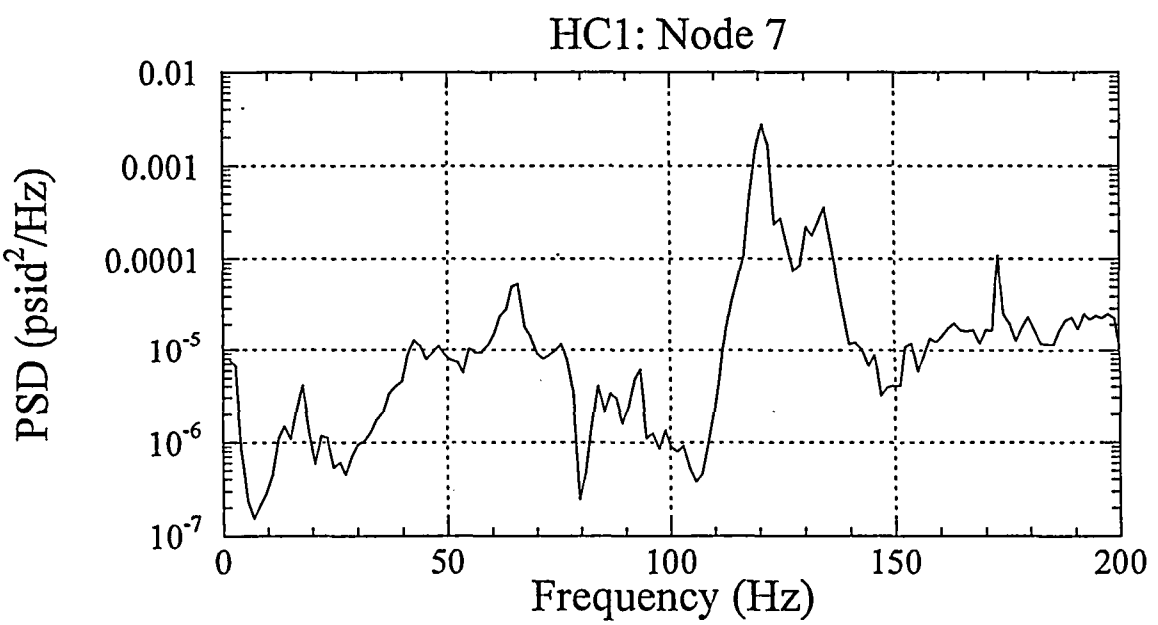

Figure 4.10. Time history and PSD of the predicted EPU pressure load (extracted from subscale tests) at the center edge of the cover plate with the outer bank hood for node 7 opposite the C-D side of the dryer.

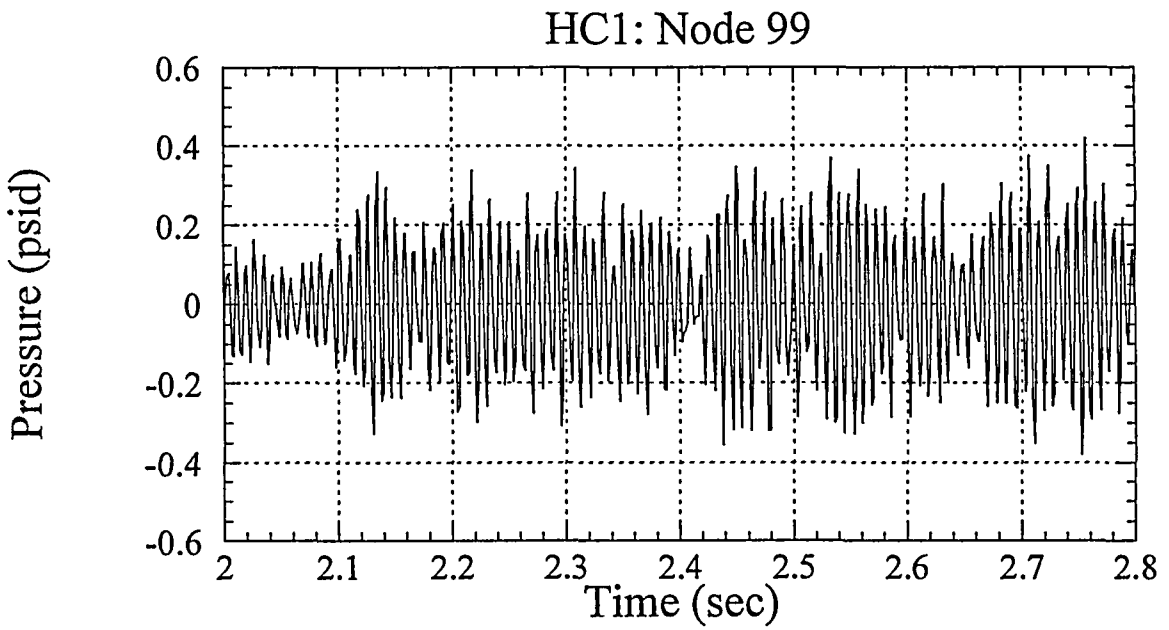

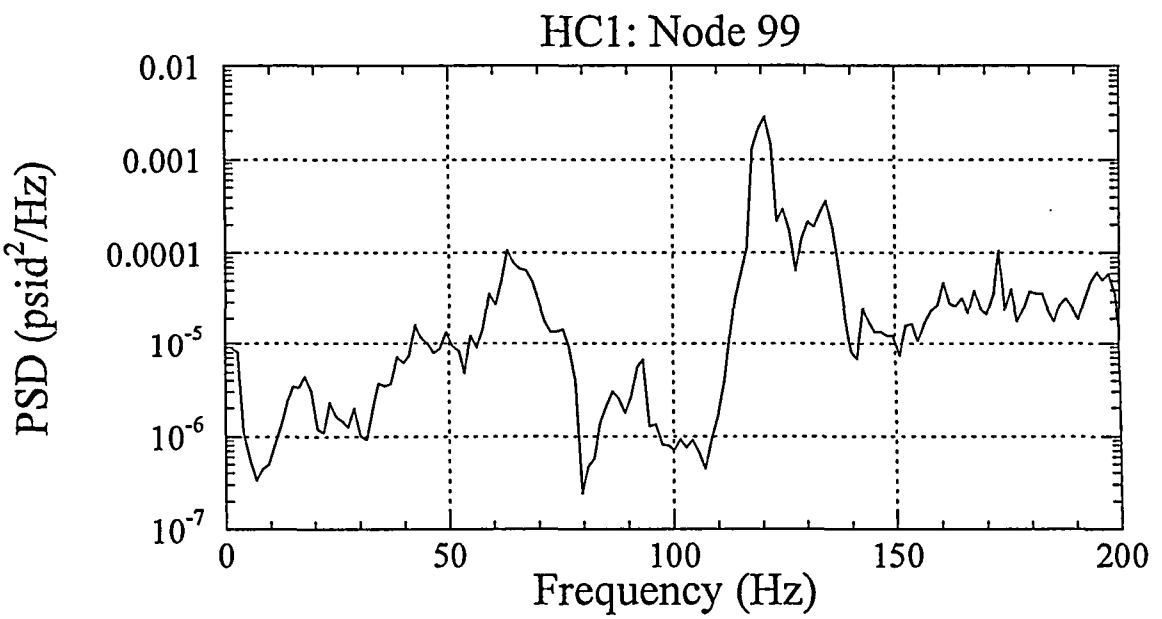

Figure 4.10 (continued). Time history and PSD of the predicted EPU pressure load (extracted from subscale tests) at the center edge of the cover plate with the outer bank hood for node 99 opposite the A-B side of the dryer.

5. Conclusions

The C.D.I. acoustic circuit analysis, using in-plant measured data from HC1, 1/8th scale measured data from C.D.I., and in-plant measured data at CLTP from SQ1:

a) Determines that steam dryer differential hydrodynamic loads at CLTP power are less than 0.18 psid, when the in-plant data are corrected by a conservatism factor determined by using the Susquehanna Unit 1 data at CLTP.

b) Suggests from the subscale data that steam dryer differential hydrodynamic loads at EPU power will be less than 0.28 psid, found by multiplying the corrected in-plant CLTP load by the increase in pressure from CLTP to EPU at subscale.

b) Predicts that the loads on dryer components are largest for components nearest the main steam line inlets and decrease inward into the reactor vessel.

c) Determines that the highest differential pressure load on the dryer occurs at 120 Hz.

The following is suggested:

- It is recommended that strain gages be fully operational when additional data at CLTP are collected and during power ascension.

6. References

1. Continuum Dynamics, Inc. 2005. Methodology to Determine Unsteady Pressure Loading on Components in Reactor Steam Domes (Rev. 6). C.D.I. Report No. 04-09 (Proprietary).

2. Continuum Dynamics, Inc. 2006. Bounding Methodology to Predict Full Scale Steam Dryer Loads from In-Plant Measurements (Rev. 1). C.D.I. Report No. 05-28 (Proprietary).

3. Structural Integrity Associates, Inc. 2006. Hope Creek Main Steam Line Strain Gage Data Reduction. Calculation File No. HC-28Q-302.

4. Continuum Dynamics, Inc. 2006. Hydrodynamic Loads at OLTP, CLTP, and 113% OLTP on Susquehanna Unit 1 Steam Dryer to 250 Hz (Rev. 0). C.D.I. Report No. 06-22.

5. Continuum Dynamics, Inc. 2006. Estimating High Frequency Flow Induced Vibration in the Main Steam Lines at Hope Creek Unit 1: A Subscale Four Line Investigation of Standpipe Behavior (Rev. 1). C.D.I. Report No. 06-16. | Rev 2

6. Continuum Dynamics, Inc. 2006. High and Low Frequency Steam Dryer Loads by Acoustic Circuit Methodology. C.D.I. Technical Memorandum No. 06-25P.

7. Continuum Dynamics, Inc. 2006. Use of One-Eighth Scale Data to Evaluate Substitution of Failed Strain Gages in In-Plant Data. C.D.I. Technical Note No. 06-26. | Rev 2